 CMES, vol.37, no.3, pp.203-242, 2008

Stable MFS Solution to Singular Direct and Inverse Problems Associated with the Laplace Equation Subjected to Noisy Data

Liviu Marin[1]

Abstract: In this paper, a meshless method for the stable solution of direct and inverse problems associated with the two-dimensional Laplace equation in the presence of boundary singularities and noisy boundary data is proposed. The governing equation and boundary conditions are discretized by the method of fundamental solutions (MFS), whilst the existence of the boundary singularity is taken into account by subtracting from the original MFS solution the corresponding singular solutions, as given by the asymptotic expansion of the solution near the singular point. However, even in the case when the boundary singularity is accounted for, the numerical solutions obtained by the direct inversion of the associated MFS linear algebraic system are still inaccurate and unstable. Therefore, the regularization of the aforementioned problems is required and this is realized by employing either the Tikhonov regularization method (TRM), or the singular value decomposition (SVD), with the corresponding optimal regularization parameter given by the L-curve method. Numerical experiments show that the proposed method is stable with respect to the noise added into the boundary data, highly accurate and computationally very efficient.

Keyword: Direct and Inverse Problems; Laplace Equation; Singularity Subtraction Technique (SST); Regularization; Method of Fundamental Solutions (MFS).

1 Introduction

In many engineering problems governed by elliptic partial differential equations, boundary singularities arise when there are sharp re-entrant corners in the boundary, the boundary conditions change abruptly, or there are discontinuities in the material properties. It is well known that these situations give rise to singularities of various types and, as a consequence, the solutions to such problems and/or

[1] Institute of Solid Mechanics, Romanian Academy, 15 Constantin Mille, Sector 1, PO Box 1-863, RO-010141 Bucharest, Romania. E-mail: marin.liviu@gmail.com

their corresponding derivatives may have unbounded values in the vicinity of the singularity. Singularities are known to affect adversely the accuracy and convergence of standard numerical methods, such as finite element (FEM), boundary element (BEM), finite-difference (FDM), spectral and meshless/meshfree methods. When the computed function is bounded, but has a branch point at the corner, the difficulty is not serious. Grid refinement and high-order discretizations are common strategies aimed at improving the convergence rate and accuracy of the above-mentioned standard methods, see e.g. Apel, Sändig and Whiteman (1996) or Apel and Nicaise (1998). If, however, the form of the singularity is taken into account and is properly incorporated into the numerical scheme then a more effective method may be constructed.

The Laplace equation arises naturally in many areas of science and engineering. For example, it is widely used to model potential problems and steady-state heat conduction. There are important studies in the literature devoted to the numerical treatment of singularities for boundary value problems related to heat conduction. Motz (1946) and Woods (1953) have investigated the removal of the singularity for the Laplace and biharmonic equations, and the Poisson equation, respectively, using the FDM. Later, Whiteman and Papamichael (1971) have employed conformal transformation methods to solve singular direct problems for the Laplace equation. Wait and Mitchell (1971) and Wait (1978) have used the FEM to stably treat singularities in the Laplace equation, whilst similar techniques, in conjunction with the BEM, have been proposed by Symm (1973), Jaswon and Symm (1977), Ingham, Heggs and Manzoor (1981), Lefeber (1989), and Ingham and Yuan (1994). Modified BEMs that take into account the singularities caused by an abrupt change in the boundary conditions and the presence of a sharp re-entrant corner in the boundary of the solution domain have been developed for the time-dependent diffusion equation and the anisotropic steady-state heat conduction problem by Lesnic, Elliott and Ingham (1995) and Mera, Elliott, Ingham and Lesnic (2002), respectively. The singular function boundary integral method has been applied for the solution of the Laplace equation in an L-shaped domain by Elliotis, Georgiou and Xenophontos (2002), and Xenophontos, Elliotis and Georgiou (2006), who have approximated the solution by the leading terms of the local solution expansion and have weakly enforced the boundary conditions by means of Lagrange multipliers. For an excellent survey on the treatment of singularities in elliptic boundary value problems, we refer the reader to Li and Lu (2000) and the references therein.

The main idea of the method of fundamental solutions (MFS), which was originally introduced by Kupradze and Aleksidze (1964) and numerically formulated for the first time by Mathon and Johnston (1977), consists of approximating the solution of the problem by a linear combination of fundamental solutions with respect to some

singularities/source points which are located outside the domain. Then the original problem is reduced to determining the unknown coefficients of the fundamental solutions and the coordinates of the source points by requiring the approximation to satisfy the boundary conditions and hence solving a nonlinear problem. If the source points are fixed *a priori* then the coefficients of the MFS approximation are determined by solving a linear problem. An excellent survey of the MFS and related methods over the past three decades has been presented by Fairweather and Karageorghis (1998).

The MFS has been successfully applied to solving a wide variety of boundary value problems. Karageorghis and Fairweather (1987) have solved numerically the biharmonic equation using the MFS. Later, their method has been modified in order to take into account the presence of boundary singularities in both the Laplace and the biharmonic equations by Karageorghis (1992) and Poullikkas, Karageorghis and Georgiou (1998). The MFS has been formulated for three-dimensional Signorini boundary value problems and it has been tested on a three-dimensional electropainting problem related to the coating of vehicle roofs in Poullikkas, Karageorghis and Georgiou (2001). Karageorghis and Fairweather (2000) have studied the use of the MFS for the approximate solution of three-dimensional isotropic materials with axisymmetrical geometry and both axisymmetrical and arbitrary boundary conditions. The application of the MFS to two-dimensional problems of steady-state heat conduction and elastostatics in isotropic and anisotropic bimaterials has been addressed by Berger and Karageorghis (1999; 2001), whilst Poullikkas, Karageorghis and Georgiou (2002) have successfully applied the MFS for solving three-dimensional elastostatics problems. Tsai (2001) has combined the dual reciprocity method (DRM) and the MFS as a meshless BEM (DRM-MFS) to solve three-dimensional Stokes flow problems by the velocity-vorticity formulation. The application of the MFS for modeling the scattering of time-harmonic electromagnetic fields, which are governed by vector Helmholtz equations with coupled boundary conditions, has been addressed by Young and Ruan (2005). Tsai, Lin, Young and Atluri (2006) have proposed a procedure for locating sources of the MFS in the case of problems without exact solutions. A novel procedure which combines the FDM and the MFS has been introduced by Hu, Young and Fan (2008) to solve numerically the nonhomogeneous diffusion problem with an unsteady forcing function. Liu (2008) has proved an equivalent relation between the modified Trefftz method (MTM) and MFS for arbitrary plane domains and, in addition, has shown that the ill-conditioning of the MFS can be alleviated through the MTM by obtaining a new system of linear equations for the corresponding modified MFS. Recently, the MFS has been successfully applied to solving inverse problems associated with the heat equation [Hon and Wei (2004; 2005); Mera,

Elliott, Ingham and Lesnic (2005); Ling and Takeuchi (2008); Marin (2008)], linear elasticity [Marin and Lesnic (2004); Marin (2005a)], steady-state heat conduction in functionally graded materials [Marin (2005b)], Helmholtz-type equations [Marin (2005c); Marin and Lesnic (2005); Jin and Zheng (2006)], and source reconstruction in steady-state heat conduction problems [Jin and Marin (2007)].

The case when exact boundary conditions for the steady-state heat conduction problem are specified on the entire boundary has been extensively studied in the literature. However, in many practical situations the boundary data are available either on the entire boundary of the solution domain or a portion of it and, when measured, they are unavoidably contaminated by inherent measurement errors. Thus the stability of the numerical method with respect to the noise added into the boundary data is of vital importance for obtaining stable, as well as physically meaningful results. The only studies that investigate the stability problems for the Laplace equations are due to Cannon (1964), Lesnic, Elliott and Ingham (1998) and Jin (2004). Cannon (1964) employed mathematical programming techniques, whilst the theory presented did not address the issue of finding higher order derivatives, and no numerical results were given to justify the theory. Lesnic, Elliott and Ingham (1998) proposed a direct method based on the BEM which yields stable and accurate results for higher-order derivatives. The MFS, in conjunction with the singular value decomposition (SVD), was utilized by Jin (2004) to stably solve the Laplace and biharmonic equations for noisy boundary data.

The objective of this paper is to propose, implement and analyse a meshless method for the accurate and stable solution of direct and inverse problems associated with the two-dimensional isotropic steady-state heat conduction (i.e. the two-dimensional Laplace equation) in the presence of boundary singularities and noisy boundary data. More precisely, the governing equation and boundary conditions are discretized by the MFS, whilst the existence of the boundary singularity is taken into account by subtracting from the original MFS solution the corresponding singular solutions, as given by the asymptotic expansion of the solution near the singular point, i.e. using the so-called singularity subtraction technique (SST). However, even in the case when the boundary singularity is accounted for, the numerical solutions obtained by the direct inversion of the associated MFS linear algebraic system are still inaccurate and unstable. Therefore, both types of problems investigated in this study need to be regularized and this is achieved by employing either the Tikhonov regularization method (TRM), or the SVD, with the regularization parameter given by the L-curve method. The proposed modified MFS, together with the aforementioned regularization methods, is then implemented for noisy direct and inverse problems in two-dimensional domains with an edge crack or a V-notch, as well as L-shaped domain. The advantages of the method proposed over other

methods, such as mesh refinement in the neighbourhood of the singularity, the use of singular BEMs and/or FEMs etc., are the high accuracy which can be obtained even when employing a small number of collocation points and sources, and the simplicity of the computational scheme. A possible drawback of the method is the difficulty in extending the method to deal with singularities in three-dimensional problems since such an extension is not straightforward.

2 General solution of the Laplace equation in polar coordinates

In this section, some well-known results on the solution of the homogeneous Laplace equation using the separation of variables in polar coordinates are revised and the notation used in the present work is introduced. Consider the steady-state heat conduction in a two-dimensional domain $\Omega \subset \mathbb{R}^2$ in the absence of heat sources. Consequently, the temperature, T, satisfies the two-dimensional Laplace equation, namely

$$\Delta \mathrm{T}(\mathbf{x}) \equiv \frac{\partial^2 \mathrm{T}(\mathbf{x})}{\partial \mathrm{x}_1^2} + \frac{\partial^2 \mathrm{T}(\mathbf{x})}{\partial \mathrm{x}_2^2} = 0, \ \mathbf{x} = (\mathrm{x}_1, \mathrm{x}_2) \in \Omega. \tag{1}$$

Let the polar coordinate system (r, θ) be defined in the usual way with respect to the Cartesian coordinates $(\mathrm{x}_1, \mathrm{x}_2) = (\mathrm{r}\cos\theta, \mathrm{r}\cos\theta)$. For $\mathrm{r} > 0$, equation (1) written in polar coordinates takes the following form:

$$\frac{\partial^2 \mathrm{T}(\mathrm{r}, \theta)}{\partial \mathrm{r}^2} + \frac{1}{\mathrm{r}} \frac{\partial \mathrm{T}(\mathrm{r}, \theta)}{\partial \mathrm{r}} + \frac{1}{\mathrm{r}^2} \frac{\partial^2 \mathrm{T}(\mathrm{r}, \theta)}{\partial \theta^2} = 0. \tag{2}$$

If we assume that the solution of equation (1) in the domain Ω can be written using the separation of variables

$$\mathrm{T}(\mathrm{r}, \theta) = f(\mathrm{r})\, g(\theta), \tag{3}$$

then the Laplace equation (1) can be recast as

$$\left(f''(\mathrm{r}) + \mathrm{r}^{-1} f'(\mathrm{r})\right) g(\theta) + \mathrm{r}^{-2} f(\mathrm{r}) g''(\theta) = 0. \tag{4}$$

If $f(\mathrm{r})\, g(\theta) \neq 0$ then the following ratio must be a constant, denoted here by λ^2:

$$\frac{f''(\mathrm{r}) + \mathrm{r}^{-1} f'(\mathrm{r})}{\mathrm{r}^{-2} f(\mathrm{r})} = -\frac{g''(\theta)}{g(\theta)} = \lambda^2, \tag{5}$$

and this results in the following two linear homogeneous ordinary differential equations with respect to the variables r and θ, respectively

$$f''(\mathrm{r}) + \mathrm{r}^{-1} f'(\mathrm{r}) - \lambda^2 \mathrm{r}^{-2} f(\mathrm{r}) = 0, \tag{6}$$

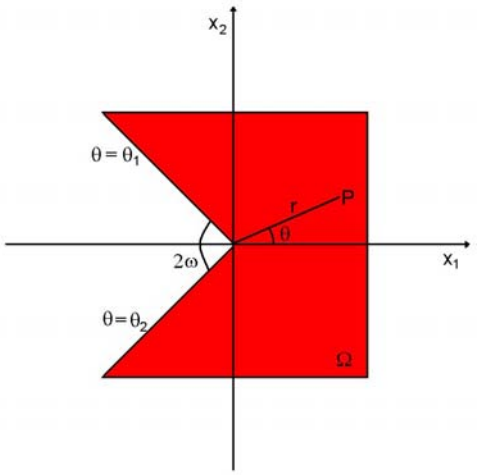

Figure 1: Schematic diagram of the two-dimensional isotropic wedge domain Ω of interior angle 2ω, $\omega \in [0, \pi)$.

$$g''(\theta) + \lambda^2 g(\theta) = 0. \tag{7}$$

For a fixed value of $\lambda > 0$, the general solutions of equations (6) and (7) are given by

$$f(\mathrm{r}) = a\mathrm{r}^{-\lambda} + b\mathrm{r}^{\lambda},\ a, b \in \mathbb{R}, \tag{8}$$

$$g(\theta) = \alpha\cos(\lambda\theta) + \beta\sin(\lambda\theta),\ \alpha, \beta \in \mathbb{R}, \tag{9}$$

respectively. Hence the general solution of equation (1) in the form (3) can be written as

$$\begin{aligned} &\mathrm{T}(\mathrm{r}, \theta) = \left(a\mathrm{r}^{-\lambda} + b\mathrm{r}^{\lambda}\right)\left[\alpha\cos(\lambda\theta) + \beta\sin(\lambda\theta)\right], \\ &a, b, \alpha, \beta \in \mathbb{R}. \end{aligned} \tag{10}$$

3 Corner singularities for the Laplace equation

Consider now that Ω is a two-dimensional isotropic wedge domain of interior angle 2ω, where $0 \leq \omega < \pi$, with the tip at the origin, O, of the local polar coordinates system and determined by two straight edges of angles θ_1 and θ_2, such that $\theta_2 - \theta_1 = 2(\pi - \omega)$, see Fig. 1. Therefore, $\Omega = \left\{\mathbf{x} \in \mathbb{R}^2 \,|0 < \mathrm{r} < \mathrm{R}(\theta), \theta_1 < \theta < \theta_2\right\}$, where $\mathrm{R}(\theta)$ is either a bounded continuous function or infinity.

In the following, we consider the boundary value problem given by equation (1) in Ω and homogeneous Neumann and/or Dirichlet boundary conditions prescribed

on the wedge edges. On taking into account the finite character of the temperature, T, in a wedge tip neighbourhood, we obtain $a = 0$ in equation (10). Hence the basis function of singular solutions to the aforementioned boundary value problem obtained from expression (10) can be written in the general form as

$$\mathrm{T}^{(\mathrm{S})}(\mathrm{r},\theta) = \mathrm{r}^{\lambda}\left[\alpha\cos(\lambda\theta) + \beta\sin(\lambda\theta)\right], \tag{11}$$

where $\alpha, \beta \in \mathbb{R}$ are unknown singular coefficients, whilst $\lambda > 0$ is referred to as the singularity exponent or eigenvalue. The singular exponent/eigenvalue, as well as the corresponding singular coefficients, are determined by the geometry and boundary conditions along the boundaries sharing the singular point.
The normal heat flux through a straight radial line defined by an angle θ and associated with the normal vector $\mathbf{n}(\theta) = (-\sin\theta, \cos\theta)$ is given by

$$\phi^{(\mathrm{S})}(\mathrm{r},\theta) = \frac{1}{\mathrm{r}}\frac{\partial}{\partial\theta}\mathrm{T}^{(\mathrm{S})}(\mathrm{r},\theta). \tag{12}$$

For the sake of convenience, the singular temperature, $\mathrm{T}^{(\mathrm{S})}$, and normal heat flux, $\phi^{(\mathrm{S})}$, given by equations (11) and (12), respectively, can be recast as:

$$\mathrm{T}^{(\mathrm{S})}(\mathrm{r},\theta) = \mathrm{r}^{\lambda}\left\{\alpha\cos[\lambda(\theta-\theta_1)] + \beta\sin[\lambda(\theta-\theta_1)]\right\}, \tag{13}$$

$$\phi^{(\mathrm{S})}(\mathrm{r},\theta) = \lambda\mathrm{r}^{\lambda-1}\left\{-\alpha\sin[\lambda(\theta-\theta_1)] + \beta\cos[\lambda(\theta-\theta_1)]\right\}. \tag{14}$$

In this study, four configurations of homogeneous Neumann (N) and Dirichlet (D) boundary conditions at the wedge edges applied to expressions (13) and (14) are considered. The conditions which allow a nontrivial solution of the resulting system of equations under the assumption $\lambda > 0$ are listed below:

Case I: N-N wedge

$$\begin{aligned} &\phi^{(\mathrm{S})}(\mathrm{r},\theta_1) = \phi^{(\mathrm{S})}(\mathrm{r},\theta_2) = 0 \Rightarrow \beta = 0 \text{ and} \\ &\sin[\lambda(\theta_2-\theta_1)] = 0 \Rightarrow \lambda = \mathrm{n}\frac{\pi}{\theta_2-\theta_1},\ \mathrm{n} \geq 0 \end{aligned} \tag{15}$$

Case II: D-D wedge

$$\begin{aligned} &\mathrm{T}^{(\mathrm{S})}(\mathrm{r},\theta_1) = \mathrm{T}^{(\mathrm{S})}(\mathrm{r},\theta_2) = 0 \Rightarrow \alpha = 0 \text{ and} \\ &\sin[\lambda(\theta_2-\theta_1)] = 0 \Rightarrow \lambda = \mathrm{n}\frac{\pi}{\theta_2-\theta_1},\ \mathrm{n} \geq 1 \end{aligned} \tag{16}$$

Case III: N-D wedge

$$\begin{aligned} &\phi^{(\mathrm{S})}(\mathrm{r},\theta_1) = \mathrm{T}^{(\mathrm{S})}(\mathrm{r},\theta_2) = 0 \Rightarrow \\ &\beta = 0 \text{ and } \cos[\lambda(\theta_2-\theta_1)] = 0 \Rightarrow \\ &\lambda = \left(\mathrm{n}-\frac{1}{2}\right)\frac{\pi}{\theta_2-\theta_1},\ \mathrm{n} \geq 1 \end{aligned} \tag{17}$$

Case IV: D-N wedge

$$\begin{aligned} &T^{(S)}(r,\theta_1) = \phi^{(S)}(r,\theta_2) = 0 \Rightarrow \\ &\alpha = 0 \text{ and } \cos[\lambda(\theta_2-\theta_1)] = 0 \Rightarrow \\ &\lambda = \left(n-\frac{1}{2}\right)\frac{\pi}{\theta_2-\theta_1},\ n \geq 1 \end{aligned} \tag{18}$$

From formulae $(15)-(18)$ it can be noticed that the singularity exponents, λ, coincide in cases I and II, and III and IV, respectively. Using the above results, the general asymptotic expansions for the singular solution of the Laplace equation for a single wedge and corresponding to homogeneous Neumann and Dirichlet boundary conditions on the wedge edges are obtained in the following form:

Case I: N-N wedge

$$\begin{aligned} &T^{(S)}(r,\theta) = \sum_{n=0}^{\infty} \alpha_n T_n^{(NN)}(r,\theta) = \sum_{n=0}^{\infty} \alpha_n r^{\lambda_n} \cos[\lambda_n(\theta-\theta_1)], \\ &\lambda_n = n\frac{\pi}{\theta_2-\theta_1},\ n \geq 0 \end{aligned} \tag{19}$$

Case II: D-D wedge

$$\begin{aligned} &T^{(S)}(r,\theta) = \sum_{n=1}^{\infty} \alpha_n T_n^{(DD)}(r,\theta) = \sum_{n=1}^{\infty} \alpha_n r^{\lambda_n} \sin[\lambda_n(\theta-\theta_1)], \\ &\lambda_n = n\frac{\pi}{\theta_2-\theta_1},\ n \geq 1 \end{aligned} \tag{20}$$

Case III: N-D wedge

$$\begin{aligned} &T^{(S)}(r,\theta) = \sum_{n=1}^{\infty} \alpha_n T_n^{(ND)}(r,\theta) = \sum_{n=1}^{\infty} \alpha_n r^{\lambda_n} \cos[\lambda_n(\theta-\theta_1)], \\ &\lambda_n = \left(n-\frac{1}{2}\right)\frac{\pi}{\theta_2-\theta_1},\ n \geq 1 \end{aligned} \tag{21}$$

Case IV: D-N wedge

$$\begin{aligned} &T^{(S)}(r,\theta) = \sum_{n=1}^{\infty} \alpha_n T_n^{(DN)}(r,\theta) = \sum_{n=1}^{\infty} \alpha_n r^{\lambda_n} \sin[\lambda_n(\theta-\theta_1)], \\ &\lambda_n = \left(n-\frac{1}{2}\right)\frac{\pi}{\theta_2-\theta_1},\ n \geq 1 \end{aligned} \tag{22}$$

In this paper, the following particular two-dimensional geometries containing a boundary singularity are investigated, see Figs. $2(a)-(c)$:

(*i*) Two-dimensional domain containing a V-notch with the re-entrant angle 2ω, $\omega \in (0,\pi/2)$, i.e. $\theta_1 = -\theta_2 = \pi - \omega$.

(*ii*) Two-dimensional domain containing an edge crack, i.e. $\theta_1 = -\theta_2 = \pi$.

(*iii*) L-shaped domain, i.e. $\theta_1 = 0$ and $\theta_2 = 3\pi/2$.

It should be mentioned that a domain containing an edge crack can also be considered as the limiting case for a domain containing a V-notch with the re-entrant angle 2ω, $\omega \in (0, \pi/2)$, in the sense that $\omega = 0$ for the aforementioned geometry. For the sake of completeness and taking into account the symmetry of the domains containing a V-notch or an edge crack, we mention that the singularity exponents corresponding to the particular geometries analysed herein are given by:

Cases I & II: N-N and D-D wedges

$$\lambda_{\mathrm{n}} = \begin{cases} \mathrm{n}\dfrac{\pi}{\pi-\omega} & \text{for a domain containing a V-notch with } \omega \in [0, \pi/2) \\ \dfrac{2\mathrm{n}}{3} & \text{for an L-shaped domain} \end{cases} \tag{23}$$

Cases III & IV: N-D and D-N wedges

$$\lambda_{\mathrm{n}} = \begin{cases} \left(\mathrm{n}-\dfrac{1}{2}\right)\dfrac{\pi}{\pi-\omega} & \text{for a domain containing a V-notch with } \omega \in [0, \pi/2) \\ \dfrac{2\mathrm{n}-1}{3} & \text{for an L-shaped domain} \end{cases} \tag{24}$$

4 Singularity subtraction technique

Consider a two-dimensional bounded domain Ω with a piecewise smooth boundary $\Gamma = \partial\Omega$ which contains a singularity at the point $\mathrm{O}(\mathbf{x}^0)$, $\mathbf{x}^0 = (\mathrm{x}_1^0, \mathrm{x}_2^0)$, that may be caused by a change in the boundary conditions and/or a re-entrant corner at O. For the simplicity of the following explanations, it is assumed that the singularity point is located at the intersection of the Dirichlet and Neumann boundary parts, see e.g. Fig. 2(c), although the method presented herein can easily be extended to other local configurations or boundary conditions. Hence the problem to be solved recasts as

$$\Delta \mathrm{T}(\mathbf{x}) \equiv \frac{\partial^2 \mathrm{T}(\mathbf{x})}{\partial \mathrm{x}_1^2} + \frac{\partial^2 \mathrm{T}(\mathbf{x})}{\partial \mathrm{x}_2^2} = 0, \quad \mathbf{x} \in \Omega \tag{25.1}$$

$$\mathrm{T}(\mathbf{x}) = \widetilde{\mathrm{T}}(\mathbf{x}), \quad \mathbf{x} \in \Gamma_{\mathrm{D}} \tag{25.2}$$

$$\phi(\mathbf{x}) \equiv \nabla \mathrm{T}(\mathbf{x}) \cdot \mathbf{n}(\mathbf{x}) = \widetilde{\phi}(\mathbf{x}), \quad \mathbf{x} \in \Gamma_{\mathrm{N}} \tag{25.3}$$

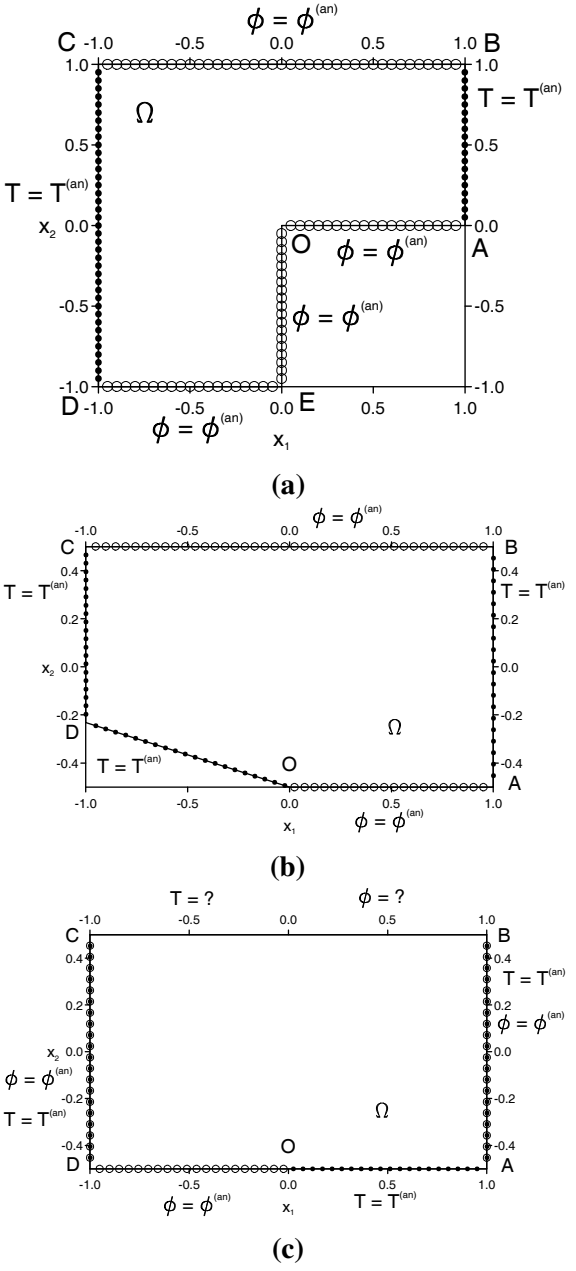

Figure 2: Schematic diagram of the geometry and boundary conditions, i.e. Dirichlet (•) and Neumann (○) conditions, respectively, corresponding to the singular problems investigated, namely (a) Example 1: N-N singular direct problem in an L-shaped domain; (b) Example 2: N-D singular direct problem in a domain containing a V-notch with the re-entrant angle $2\omega = \pi/6$; and (c) Example 3: D-N singular inverse problem in a domain containing an edge crack OD.

where $\Gamma_D \neq \emptyset$, $\Gamma_N \neq \emptyset$, $\overline{\Gamma}_D \cup \overline{\Gamma}_N \subset \Gamma$, $\{O\} \subset \overline{\Gamma}_D \cap \overline{\Gamma}_N$, $\widetilde{T}$ and $\widetilde{\phi}$ are prescribed boundary temperature and normal heat flux, respectively, and we denote the closure of a set by an overbar. It should be noted that the above formulation of the boundary value problem associated with the isotropic steady-state heat conduction (25.1) – (25.3) is very general, in the sense that it contains both the direct and inverse problems. More precisely, the following situations may occur:

1. Direct problem: $\overline{\Gamma}_D \cup \overline{\Gamma}_N = \Gamma$ and $\Gamma_D \cap \Gamma_N = \emptyset$;
2. Inverse problem: $\overline{\Gamma}_D \cup \overline{\Gamma}_N \subset \Gamma$ and $\Gamma_D \cap \Gamma_N \neq \emptyset$.

Moreover, we also assume that the Dirichlet, $\widetilde{T}\big|_{\Gamma_D}$, and Neumann, $\widetilde{\phi}\big|_{\Gamma_N}$, input data have been perturbed as

$$\widetilde{T}^{\varepsilon}\big|_{\Gamma_D} = \widetilde{T}\big|_{\Gamma_D} + \delta T, \qquad \widetilde{\phi}^{\varepsilon}\big|_{\Gamma_N} = \widetilde{\phi}\big|_{\Gamma_N} + \delta\phi, \tag{26}$$

where $\delta\widetilde{T}$ and $\delta\widetilde{\phi}$ are Gaussian random variables with mean zero and standard deviations $\sigma_T = \max_{\Gamma_D} |T| \times (p_T/100)$ and $\sigma_\phi = \max_{\Gamma_N} |\phi| \times (p_\phi/100)$, respectively, generated by the NAG subroutine G05DDF, and p_T and p_ϕ are the percentages of additive noise included into the input data $T\big|_{\Gamma_D}$ and $\phi\big|_{\Gamma_N}$ in order to simulate the inherent measurement errors.

In order to avoid numerical difficulties arising from the presence of the singularity in the potential solution at O, it is convenient to modify the original problem before it is solved by the MFS. Due to the linearity of the Laplace operator and the boundary conditions, the superposition principle is valid and the temperature, T, and the normal heat flux, ϕ, can be written as

$$T(\mathbf{x}) = \underbrace{\left(T(\mathbf{x}) - T^{(S)}(\mathbf{x})\right)}_{\equiv T^{(R)}(\mathbf{x})} + T^{(S)}(\mathbf{x}), \quad \mathbf{x} \in \overline{\Omega}, \tag{27}$$

$$\phi(\mathbf{x}) = \underbrace{\left(\phi(\mathbf{x}) - \phi^{(S)}(\mathbf{x})\right)}_{\equiv \phi^{(R)}(\mathbf{x})} + \phi^{(S)}(\mathbf{x}), \quad \mathbf{x} \in \Gamma, \tag{28}$$

where $T^{(S)}(\mathbf{x})$ is a particular singular potential solution of the original problem (25.1) – (25.3) which satisfies the corresponding homogeneous boundary conditions on the parts of the boundary containing the singularity point O and $\phi^{(S)}(\mathbf{x}) \equiv \nabla T^{(S)}(\mathbf{x}) \cdot \mathbf{n}(\mathbf{x})$ is its conormal derivative. If appropriate functions are chosen for the singular temperature and its conormal derivative then the numerical analysis can be carried out for the regular potential solution $T^{(R)}(\mathbf{x})$ and its conormal derivative

$\phi^{(\mathrm{R})}(\mathbf{x}) \equiv \nabla \mathrm{T}^{(\mathrm{R})}(\mathbf{x}) \cdot \mathbf{n}(\mathbf{x})$ only. In terms of the regular potential solution $\mathrm{T}^{(\mathrm{R})}(\mathbf{x})$, the original problem (25.1)-(25.3) becomes

$$\Delta \mathrm{T}^{(\mathrm{R})}(\mathbf{x}) = 0, \quad \mathbf{x} \in \Omega \tag{29.1}$$

$$\mathrm{T}^{(\mathrm{R})}(\mathbf{x}) = \widetilde{\mathrm{T}}^{\varepsilon}(\mathbf{x}) - \mathrm{T}^{(\mathrm{S})}(\mathbf{x}), \quad \mathbf{x} \in \Gamma_{\mathrm{D}} \tag{29.2}$$

$$\phi^{(\mathrm{R})}(\mathbf{x}) = \widetilde{\phi}^{\varepsilon}(\mathbf{x}) - \phi^{(\mathrm{S})}(\mathbf{x}), \quad \mathbf{x} \in \Gamma_{\mathrm{N}} \tag{29.3}$$

The modified boundary conditions (29.2) and (29.3) introduce additional unknowns into the problem, which are the constants of the particular potential solution used to represent the singular potential solution. It should be noted that these constants are similar to the stress intensity factors corresponding to an analogous problem for the Lamé (or Navier) system and, in what follows, they will be referred to as flux intensity factors. Since the flux intensity factors are unknown at this stage of the problem, they become primary unknowns.

In order to obtain a unique solution to the regular problem $(29.1)-(29.3)$, it is necessary to specify additional constraints which must be as many as the number of the unknown flux intensity factors, i.e. one for each singular solution/eigenfunction included in the analysis. These extra conditions must be applied in such a way that the cancelation of the singularity in the regular potential solution is ensured. This is achieved by constraining the regular solution and/or its conormal derivative directly in a neighbourhood of the singularity point O

$$\mathrm{T}^{(\mathrm{R})}(\mathbf{x}) = 0, \quad \mathbf{x} \in \Gamma_{\mathrm{N}} \cap \mathrm{B}(\mathrm{O}; \tau) \tag{30.1}$$

and/or

$$\phi^{(\mathrm{R})}(\mathbf{x}) = 0, \quad \mathbf{x} \in \Gamma_{\mathrm{D}} \cap \mathrm{B}(\mathrm{O}; \tau), \tag{30.2}$$

where $\mathrm{B}(\mathrm{O}; \tau) = \left\{ \mathbf{x} \in \mathbb{R}^2 \,\middle|\, \|\mathbf{x} - \mathbf{x}^0\| < \tau \right\}$, $\tau > 0$ is sufficiently small and $\|\cdot\|$ represents the Euclidean norm.

For example, for the problem $(29.1)-(29.3)$ the singular solution and its normal derivative are expressed, in terms of the polar coordinates (r, θ), as

$$\begin{aligned} \mathrm{T}^{(\mathrm{S})}(\mathbf{x}) &\equiv \mathrm{T}^{(\mathrm{S})}(\mathrm{r}, \theta) = \sum_{\mathrm{n}=1}^{\mathrm{n_S}} \alpha_{\mathrm{n}} \mathrm{T}_{\mathrm{n}}^{(\mathrm{DN})}(\mathrm{r}, \theta), \\ \phi^{(\mathrm{S})}(\mathbf{x}) &\equiv \phi^{(\mathrm{S})}(\mathrm{r}, \theta) = \sum_{\mathrm{n}=1}^{\mathrm{n_S}} \alpha_{\mathrm{n}} \phi_{\mathrm{n}}^{(\mathrm{DN})}(\mathrm{r}, \theta), \end{aligned} \tag{31}$$

where $\mathrm{T}_{\mathrm{n}}^{(\mathrm{DN})}(\mathrm{r}, \theta)$ is given by equation (22), $\phi_{\mathrm{n}}^{(\mathrm{DN})}(\mathrm{r}, \theta)$ is obtained by taking the conormal derivative of $\mathrm{T}_{\mathrm{n}}^{(\mathrm{DN})}(\mathrm{r}, \theta)$ and α_{n}, $\mathrm{n} = 1, \ldots, \mathrm{n_S}$, are the unknown flux intensity factors.

5 The method of fundamental solutions

The fundamental solution of the two-dimensional Laplace equation is given by, see e.g. Berger and Karageorghis (1999),

$$\mathscr{F}(\mathbf{x},\mathbf{y}) = \frac{1}{2\pi}\,\ln\frac{1}{\|\mathbf{x}-\mathbf{y}\|}, \quad \mathbf{x}\in\overline{\Omega}, \quad \mathbf{y}\in\mathbb{R}^2\setminus\overline{\Omega}, \tag{32}$$

where $\mathbf{x} = (x_1, x_2)$ is either a boundary or a domain point and $\mathbf{y} = (y_1, y_2)$ is a source point.

According to the MFS approach, the regular temperature, $T^{(R)}$, in the solution domain is approximated by a linear combination of fundamental solutions with respect to M source points $\mathbf{y}^j$ in the form

$$T^{(R)}(\mathbf{x}) \approx \sum_{j=1}^{M} c_j\,\mathscr{F}(\mathbf{x},\mathbf{y}^j), \quad \mathbf{x}\in\overline{\Omega}, \tag{33}$$

where $\mathbf{c}_j \in \mathbb{R}$, $j = 1,\ldots,M$, are the unknown coefficients. Then the regular normal heat flux on the boundary Γ can be approximated by

$$\phi^{(R)}(\mathbf{x}) \approx \sum_{j=1}^{M} c_j\,\mathscr{G}(\mathbf{x},\mathbf{y}^j), \quad \mathbf{x}\in\Gamma, \tag{34}$$

where $\mathscr{G}(\mathbf{x},\mathbf{y}) = \nabla_{\mathbf{x}}\mathscr{F}(\mathbf{x},\mathbf{y})\cdot\mathbf{n}(\mathbf{x})$ is given by

$$\mathscr{G}(\mathbf{x},\mathbf{y}) = -\frac{(\mathbf{x}-\mathbf{y})^T\cdot\mathbf{n}(\mathbf{x})}{2\pi\,\|\mathbf{x}-\mathbf{y}\|^2}, \quad \mathbf{x}\in\Gamma, \quad \mathbf{y}\in\mathbb{R}^2\setminus\overline{\Omega}. \tag{35}$$

Assume that the singular point O is located between the collocation points $\mathbf{x}^{n_D^0}\in\Gamma_D$ and $\mathbf{x}^{n_N^0}\in\Gamma_N$, see also Fig. 2(c), and n_S singular solutions/eigenfunctions, $T_n^{(DN)}(r,\theta)$, as well as flux intensities, α_n, are taken into account, such that the additional constraints for the regular temperature and/or its conormal derivative given by equation (30.1) and (30.2), respectively, read as

$$T^{(R)}(\mathbf{x}^{n_N^0+1-m}) = 0, \quad i = 2m-1 \in \{1,\ldots,n_S\}, \tag{36}$$

and

$$\phi^{(R)}(\mathbf{x}^{n_D^0-1+m}) = 0, \quad i = 2m \in \{1,\ldots,n_S\}. \tag{37}$$

If n_D collocation points $\mathbf{x}^i$, $i = 1,\ldots,n_D$, and n_N collocation points $\mathbf{x}^{n_D+i}$, $i = 1,\ldots,n_N$, are chosen on the boundaries Γ_D and Γ_N, respectively, such that $N =$

$n_D + n_N$, and the location of the source points $\mathbf{y}^j$, $j = 1, \ldots, M$, is set then the boundary value problem $(29.1) - (29.3)$, together with the additional conditions (30), recasts as a system of $(N + n_S)$ linear algebraic equations with $(M + n_S)$ unknowns which can be generically written as

$$\mathbf{A}\,\widetilde{\mathbf{c}} = \mathbf{F}, \tag{38}$$

where $\widetilde{\mathbf{c}} = (c_1, \ldots, c_M, \alpha_1, \ldots, \alpha_{n_S}) \in \mathbb{R}^{M+n_S}$ and the components of the MFS matrix $\mathbf{A} \in \mathbb{R}^{(N+n_S)\times(M+n_S)}$ and right-hand side vector $\mathbf{F} \in \mathbb{R}^{N+n_S}$ are given by

$$A_{ij} = \begin{cases} \mathscr{F}(\mathbf{x}^i, \mathbf{y}^j), & i = \overline{1, n_D}, \quad j = \overline{1, M} \\ T^{(DN)}_{j-M}(r^i, \theta^i), & i = \overline{1, n_D}, \quad j = \overline{(M+1), (M+n_S)} \\ \mathscr{G}(\mathbf{x}^i, \mathbf{y}^j), & i = \overline{(n_D+1), (n_D+n_N)}, \quad j = \overline{1, M} \\ \phi^{(DN)}_{j-M}(r^i, \theta^i), & i = \overline{(n_D+1), (n_D+n_N)}, \quad j = \overline{(M+1), (M+n_S)} \\ \mathscr{F}(\mathbf{x}^{n^0_N+1-m-N}, \mathbf{y}^j), & i - N = 2m - 1 = \overline{1, n_S}, \quad j = \overline{1, M} \\ \mathscr{G}(\mathbf{x}^{n^0_D-1+m-N}, \mathbf{y}^j), & i - N = 2m = \overline{1, n_S}, \quad j = \overline{1, M} \\ 0, & i - N = \overline{1, n_S}, \quad j = \overline{(M+1), (M+n_S)} \end{cases} \tag{39}$$

$$F_i = \begin{cases} \widetilde{T}^{\varepsilon}(\mathbf{x}^i), & i = \overline{1, n_D} \\ \widetilde{\phi}^{\varepsilon}(\mathbf{x}^i), & i = \overline{(n_D+1), (n_D+n_N)} \\ 0, & i = \overline{(n_D+n_N+1), (n_D+n_N+n_S)} \end{cases} \tag{40}$$

It should be noted that in order to uniquely determine the solution $\widetilde{\mathbf{c}}$ of the system of linear algebraic equations (38), i.e. the coefficients c_j, $j = 1, \ldots, M$, in approximations (33) and (34) and the flux intensity factors α_n, $n = 1, \ldots, n_S$, in the asymptotic expansions (31), the total number of collocation points corresponding to the Dirichlet and Neumann boundary conditions, N, and the number of source points, M, must satisfy the inequality $M \leq N$.

In order to implement the MFS, the location of the source points has to be determined and this is usually achieved by considering either the static or the dynamic approach. In the static approach, the source points are pre-assigned and kept fixed throughout the solution process, whilst in the dynamic approach, the source points and the unknown coefficients are determined simultaneously during the solution process, see Fairweather and Karageorghis (1998). For nonlinear systems, the uniqueness of the solution is not always guaranteed and it is computationally much more expensive. In addition, the discretised MFS system is severely ill-posed in the

case of inverse problems and thus the dynamic approach transforms the problem into a more difficult nonlinear ill-posed problem. The dynamic approach results in a system of nonlinear equations, which may be solved using minimization methods. Alternatively, Tankelevich, Fairweather, Karageorghis and Smyrlis (2006), consider the source points located on a so-called pseudo-boundary, which has the same shape as the boundary of the domain, and the problem is solved for a sequence of such pseudo-boundaries, whilst the optimal pseudo-boundary is taken to be the one for which boundary conditions are satisfied most accurately. From a computational point of view, the dynamic approach might not be appropriate for inverse problems with noisy data. Moreover, Mitic and Rashed (2004) have shown that the distribution and number of the source points are not, in general, important under certain conditions, in the sense that the number of sources should reflect the degrees of freedom inherent in the boundary conditions of the problem. Hence the dynamic approach for determining the optimal location of the source points might be unnecessary. Therefore, we have decided to employ the static approach in our computations with the source points located on a pseudo-boundary chosen in the same manner as Tankelevich, Fairweather, Karageorghis and Smyrlis (2006).

6 Regularization

The MFS can be regarded as a Fredholm integral equation of the first kind with an analytical kernel function, see e.g. Golberg and Chen (1999), which is severely ill-posed according to the theory of integral equations. Consequently, as an approximation to the integral operator, the discretisation matrix $\mathbf{A}$ is severely ill-conditioned. The accurate and stable solution of equation (38) is very important for obtaining physically meaningful numerical results. Regularization methods are among the most popular and successful methods for solving stably and accurately ill-conditioned matrix equations, see Hansen (1998) and Tikhonov and Arsenin (1986). In our computations, we use both the SVD and the TRM to solve the matrix equation arising from the MFS discretisation.

6.1 Singular Value Decomposition (SVD)

The SVD of a matrix $\mathbf{A} \in \mathbb{R}^{(N+n_S)\times(M+n_S)}$, $M \leq N$, is given by, see e.g. Hansen (1998),

$$\mathbf{A} = \mathbf{U}\boldsymbol{\Sigma}\mathbf{V}^{T}, \tag{41}$$

where $\mathbf{U} = [\mathbf{u}_1, \mathbf{u}_2, \ldots, \mathbf{u}_{N+n_S}]$ and $\mathbf{V} = [\mathbf{v}_1, \mathbf{v}_2, \ldots, \mathbf{v}_{M+n_S}]$ are orthonormal matrices with column vectors called the left and the right singular vectors, respectively, T denotes the matrix transposition and $\boldsymbol{\Sigma} = \mathrm{diag}(\sigma_1, \sigma_2, \ldots, \sigma_{M+n_S})$ is a diagonal matrix with nonnegative diagonal elements in non-increasing order, which are the singular values of $\mathbf{A}$.

On using the SVD, the solution $\mathbf{c}$ to the matrix equation (38) can be succinctly written as a linear combination of the right singular vectors, namely

$$\widetilde{\mathbf{c}} = \sum_{i=1}^{\text{rank}(\mathbf{A})} \frac{\mathbf{u}_i^T \mathbf{F}}{\sigma_i} \mathbf{v}_i, \tag{42}$$

where $\text{rank}(\mathbf{A})$ is the rank of the matrix $\mathbf{A}$. For an ill-conditioned matrix equation, there are many small singular values clustering around zero and therefore the solution obtained by standard methods, such as the Gauss elimination method, may be dominated by the contribution of the small singular values and hence it becomes unbounded and oscillatory. One simple remedy is to truncate the above summation, i.e. by considering an approximate solution, $\mathbf{c}_n$, given by

$$\widetilde{\mathbf{c}}_n = \sum_{i=1}^{n} \frac{\mathbf{u}_i^T \mathbf{F}}{\sigma_i} \mathbf{v}_i, \tag{43}$$

where $n \leq \text{rank}(\mathbf{A})$ is the regularization parameter which determines when one starts to leave out small singular values. This method is known as the SVD in the inverse problem community, see Hansen (1998).

6.2 The Tikhonov Regularization Method (TRM)

The Tikhonov regularized solution to the system of linear algebraic equations (38) is sought as, see Tikhonov and Arsenin (1986),

$$\widetilde{\mathbf{c}}_\lambda : \mathscr{T}_\lambda(\widetilde{\mathbf{c}}) = \min_{\widetilde{\mathbf{c}} \in \mathbb{R}^{M+n_S}} \mathscr{T}_\lambda(\widetilde{\mathbf{c}}), \tag{44}$$

where $\mathscr{T}_\lambda$ represents the zeroth-order Tikhonov functional given by

$$\begin{aligned} &\mathscr{T}_\lambda(\cdot) : \mathbb{R}^{M+n_S} \longrightarrow [0,\infty), \\ &\mathscr{T}_\lambda(\widetilde{\mathbf{c}}) = \|\mathbf{A}\widetilde{\mathbf{c}} - \mathbf{F}\|^2 + \lambda^2 \|\widetilde{\mathbf{c}}\|^2, \end{aligned} \tag{45}$$

and $\lambda > 0$ is the regularization parameter to be chosen. Formally, the Tikhonov regularized solution $\widetilde{\mathbf{c}}_\lambda$ of the problem (44) is given as the solution of the normal equation

$$\left(\mathbf{A}^T\mathbf{A} + \lambda^2 \mathbf{I}_{M+n_S}\right)\widetilde{\mathbf{c}} = \mathbf{A}^T\mathbf{F}, \tag{46}$$

where $\mathbf{I}_{M+n_S}$ is the identity matrix. If the right-hand side of equation (38) is corrupted by noise, i.e.

$$\|\mathbf{F} - \mathbf{F}^\delta\| \leq \delta, \tag{47}$$

then the following stability estimate holds, see Engl, Hanke and Neubauer (2000),

$$\|\widetilde{\mathbf{c}}_\lambda - \widetilde{\mathbf{c}}_\lambda^\delta\| \leq \frac{\delta}{\lambda}, \tag{48}$$

where

$$\widetilde{\mathbf{c}}_\lambda = \left(\mathbf{A}^{\mathrm{T}}\mathbf{A} + \lambda^2 \mathbf{I}_{\mathrm{M+n_S}}\right)^{-1} \mathbf{A}^{\mathrm{T}}\mathbf{F}. \tag{49}$$

6.3 The L-Curve Method

The performance of regularization methods depends crucially on the suitable choice of the regularization parameter. One extensively studied criterion is the discrepancy principle, see e.g. Morozov (1966). Although this criterion is mathematically rigorous, it requires a reliable estimation of the amount of noise added into the data which may not be available in practical problems. Heuristical approaches are preferable in the case when no *a priori* information about the noise is available. For both the TRM and SVD, several heuristical approaches have been proposed, including the L-curve criterion, see Hansen (1998), and the generalized cross-validation, see Wahba (1977). In this paper, we employ the L-curve criterion to determine the optimal regularization parameter for the regularization methods investigated, i.e. the optimal truncation number, $\mathrm{n_{opt}}$, in the case of the SVD and the optimal regularization parameter, λ_{opt}, in the case of the TRM, see Hansen (1998).

If we define on a logarithmic scale the curves

$$\{(\|\mathbf{A}\widetilde{\mathbf{c}}_\mathrm{n} - \mathbf{F}\|, \|\widetilde{\mathbf{c}}_\mathrm{n}\|) \,|\, \mathrm{n} = 1, 2, \ldots, \mathrm{rank}(\mathbf{A})\} \text{ and } \{(\|\mathbf{A}\widetilde{\mathbf{c}}_\lambda - \mathbf{F}\|, \|\widetilde{\mathbf{c}}_\lambda\|) \,|\, \lambda > 0\}$$

for the SVD and TRM, respectively, then these typically have an L-shaped form and hence they are referred to as L-curves. According to the L-curve criterion, the optimal regularization parameter corresponds to the corner of the L-curve since a good tradeoff between the residual and solution norms is achieved at this point. Numerically, the L-curve method is robust and stable with respect to both uncorrelated and highly correlated noise. Furthermore, this criterion works effectively with certain classes of practical problems, see Hansen (1998) and Chen, Chen, Hong and Chen (1995). For a discussion of the theoretical aspects of the L-curve criterion, we refer the reader to Hanke (1996) and Vogel (1996).

Several algorithms for locating the corner of the L-curve have been reported in the literature, see e.g. Hansen (1998), Guerra and Hernandez (2001), Kaufman and Neumaier (1996) and Castellanos, Gomez and Guerra (2002). The first procedure is based on fitting a parametric cubic spline to the discrete points and then taking the point corresponding to the maximum curvature of the L-curve to be its corner [Hansen (1998)]. The second algorithm employs a conic to fit the set of

discrete points [Guerra and Hernandez (2001)], whilst the third one is based on using a linear-linear scale and inverting the axis [Kaufman and Neumaier (1996)]. All these procedures need to check the monotonicity condition for the sequences of the residual and solution norms, and discard those points where the monotonicity condition is not fulfilled. The last algorithm, namely the triangle method, is based on geometric considerations [Castellanos, Gomez and Guerra (2002)]. In the present study, we mainly employ the first algorithm. However, the curvature of the parametric spline is very sensitive to the distribution of the collocation points and occasionally the located corner is not suitable, see Hansen (1998). Therefore, visual inspection is used as an auxiliary procedure.

7 Numerical results and discussion

It is the purpose of this section to present the performance of the MFS+SST, in conjunction with either the TRM or SVD. To do so, we solve numerically both the direct and inverse boundary value problems $(25.1)-(25.3)$ associated with the two-dimensional isotropic steady-state heat conduction subjected to noisy boundary data and boundary singularities.

7.1 Examples

In the case of the singular boundary value problems for the Laplace equation with noisy data analysed herein, the solution domains under consideration, Ω, accessible boundaries, Γ_{D} and Γ_{N}, and corresponding analytical solutions for the temperature, $\mathrm{T}^{(\mathrm{an})}(\mathbf{x})$, are given as follows:

Example 1. N-N singular direct problem for an L-shaped domain, see Fig. 2(a):

$$\Omega = \mathrm{OABCDE} = (-1.0,1.0)\times(0.0,1.0)\cup(-1.0,0.0)\times(-1.0,0.0] \tag{50.1}$$

$$\Gamma_{\mathrm{D}} = \mathrm{AB}\cup\mathrm{CD} = \{1.0\}\times(0.0,1.0)\cup\{-1.0\}\times(-1.0,1.0) \tag{50.2}$$

$$\begin{aligned}\Gamma_{\mathrm{N}} =& \mathrm{OA}\cup\mathrm{BC}\cup\mathrm{DE}\cup\mathrm{EO}\\ =&(0.0,1.0)\times\{0.0\}\cup(-1.0,1.0)\times\{1.0\}\cup(-1.0,0.0)\times\{0.0\}\\ &\cup\{0.0\}\times(-1.0,0.0)\end{aligned} \tag{50.3}$$

$$\mathrm{T}^{(\mathrm{an})}(\mathbf{x}) = 5.00+2.50\mathrm{T}_2^{(\mathrm{NN})}(\mathbf{x})-1.50\mathrm{T}_3^{(\mathrm{NN})}(\mathbf{x})-2.00\mathrm{T}_4^{(\mathrm{NN})}(\mathbf{x}),\ \mathbf{x}\in\overline{\Omega} \tag{50.4}$$

Example 2. N-D singular direct problem for a rectangle containing a V-notch with the re-entrant angle $2\omega=\pi/6$ (Motz-type problem), see Fig. 2(b):

$$\Omega = \mathrm{OABCD} = (-1.0,1.0)\times(-0.5,0.5)\setminus\Delta\mathrm{ODD}' \tag{51.1}$$

$$\begin{aligned}\Gamma_{\mathrm{D}} =& \mathrm{AB}\cup\mathrm{CD}\cup\mathrm{DO}\\ =& \{1.0\}\times(-0.5,0.5)\cup\{-1.0\}\times(-0.5+\sin\omega,0.5)\\ &\cup\{(-l,-0.5+l\sin\omega)\,|0<l<1\}\end{aligned} \tag{51.2}$$

$$\Gamma_{\mathrm{N}} = \mathrm{OA}\cup\mathrm{BC} = (0.0,1.0)\times\{-0.5\}\cup(-1.0,1.0)\times\{-0.5\} \tag{51.3}$$

$$\mathrm{T}^{(\mathrm{an})}(\mathbf{x}) = 3.00+1.50\,\mathrm{T}_2^{(\mathrm{ND})}(\mathbf{x}) \qquad +1.00\,\mathrm{T}_4^{(\mathrm{ND})}(\mathbf{x}), \quad \mathbf{x}\in\overline{\Omega} \tag{51.4}$$

Example 3. D-N singular inverse problem for a rectangle containing an edge crack, see Fig. 2(c):

$$\Omega = \mathrm{ABCD} = (-1.0,1.0)\times(-0.5,0.5) \tag{52.1}$$

$$\begin{aligned}\Gamma_{\mathrm{D}} =& \mathrm{OA}\cup\mathrm{AB}\cup\mathrm{CD}\\ =& (0.0,1.0)\times\{-0.5\}\cup\{-1.0,1.0\}\times(-0.5,0.5)\end{aligned} \tag{52.2}$$

$$\begin{aligned}\Gamma_{\mathrm{N}} =& \mathrm{AB}\cup\mathrm{CD}\cup\mathrm{DO}\\ =& \{-1.0,1.0\}\times(-0.5,0.5)\cup(-1.0,0.0)\times\{-0.5\}\end{aligned} \tag{52.3}$$

$$\mathrm{T}^{(\mathrm{an})}(\mathbf{x}) = 5.00+2.50\mathrm{T}_1^{(\mathrm{DN})}(\mathbf{x})-1.50\mathrm{T}_3^{(\mathrm{DN})}(\mathbf{x})-2.00\mathrm{T}_4^{(\mathrm{DN})}(\mathbf{x}),\ \mathbf{x}\in\overline{\Omega} \tag{52.4}$$

It should be mentioned that all examples analysed in this study contain a singularity at the point $\mathrm{O}(\mathbf{x}^0)$, where $\mathbf{x}^0=(0.0,0.0)$ for Example 1 and $\mathbf{x}^0=(0.0,-0.5)$ in the case of Examples 2 and 3. Moreover, this singularity is caused by the nature of the analytical solutions for the temperatures considered, i.e. the analytical temperature solutions are given as linear combinations of the first four singular solutions/eigenfunctions satisfying homogeneous boundary conditions on the edges of the wedge, as well as by a sharp corner in the boundary (Examples 1 and 2) or by an abrupt change in the boundary conditions at O (Example 3), see Figs. 2(a)-(c). In the case of Example 3, which corresponds to an inverse problem, it can be seen that the boundary $\Gamma_{\mathrm{D}}\cap\Gamma_{\mathrm{N}}=\mathrm{AB}\cup\mathrm{CD}$ is over-specified by prescribing on it both the temperature, $\mathrm{T}|_{\mathrm{AB}\cup\mathrm{CD}}$, and normal heat flux, $\phi|_{\mathrm{AB}\cup\mathrm{CD}}$, whilst the boundary BC is under-specified since neither the temperature, $\mathrm{T}|_{\mathrm{BC}}$, nor the normal heat flux, $\phi|_{\mathrm{BC}}$, is known and has to be determined.

The singular boundary value problems investigated in this paper have been solved using a uniform distribution of both the boundary collocation points $\mathbf{x}^{\mathrm{i}}$, $\mathrm{i}=1,\ldots,\mathrm{N}$, and the source points $\mathbf{y}^{\mathrm{j}}$, $\mathrm{j}=1,\ldots,\mathrm{M}$, with the mention that the later were located on a so-called pseudo-boundary, which has the same shape as the boundary Γ of the solution domain and is situated at the distance $d>0$ form Γ, see e.g. Tankelevich, Fairweather, Karageorghis and Smyrlis (2006). Furthermore, the number of boundary collocation points was set to:

(*i*) $N = 154$ for Example 1, such that 19 and 39 collocation points are situated on each of the boundaries OA, AB, DE and EO, and BC and CD, respectively;

(*ii*) $N = 120$ for Examples 2 and 3, such that $N/3 = 40$ and $N/6 = 20$ collocation points are situated on each of the boundaries BC and OA, AB, CD and OD, respectively.

In addition, for all examples investigated throughout this study, the number of source points, M, was taken to be equal to that of the boundary collocation points, N, i.e. $M = N$.

7.2 Accuracy errors

In what follows, we denote by $T^{(num)}$ and $\phi^{(num)}$ the numerical solutions for the temperature and normal heat flux, respectively, obtained using the least-squares method (LSM), i.e. by a direct inversion method, TRM and SVD, i.e. by regularization methods, and by subtracting the first $n_S \geq 0$ singular solutions/eigenfunctions, with the convention that when $n_S = 0$ then the numerical temperature and normal heat flux are obtained using the standard MFS, i.e. without removing the singularity.

In order to measure the accuracy of the numerical approximation for the temperature, $T^{(num)}$, and normal heat flux, $\phi^{(num)}$, with respect to their corresponding analytical values, $T^{(an)}$, and , $\phi^{(an)}$, respectively, we define the *relative root mean-square* (*RMS*) *errors* by

$$e_T(\Gamma_j) = \sqrt{\sum_{j=1}^{N_j} \left(T^{(num)}(\mathbf{x}^j) - T^{(an)}(\mathbf{x}^j)\right)^2 \Bigg/ \sum_{j=1}^{N_j} \left(T^{(an)}(\mathbf{x}^j)\right)^2} \tag{53}$$

$$e_\phi(\Gamma_j) = \sqrt{\sum_{j=1}^{N_j} \left(\phi^{(num)}(\mathbf{x}^j) - \phi^{(an)}(\mathbf{x}^j)\right)^2 \Bigg/ \sum_{j=1}^{N_j} \left(\phi^{(an)}(\mathbf{x}^j)\right)^2} \tag{54}$$

where N_j is the number of collocation points on the boundary $\Gamma_j \subset \Gamma$. Furthermore, we also define the *normalized errors*

$$\begin{aligned} \mathrm{err}\left(T(\mathbf{x})\right) &= \frac{|T^{(num)}(\mathbf{x}) - T^{(an)}(\mathbf{x})|}{\max\limits_{\mathbf{y}\in\widetilde{\Gamma}} |T^{(an)}(\mathbf{y})|}, \quad \mathbf{x} \in \Gamma, \\ \mathrm{err}\left(\phi(\mathbf{x})\right) &= \frac{|\phi^{(num)}(\mathbf{x}) - \phi^{(an)}(\mathbf{x})|}{\max\limits_{\mathbf{y}\in\widetilde{\Gamma}} |\phi^{(an)}(\mathbf{y})|}, \quad \mathbf{x} \in \Gamma, \end{aligned} \tag{55}$$

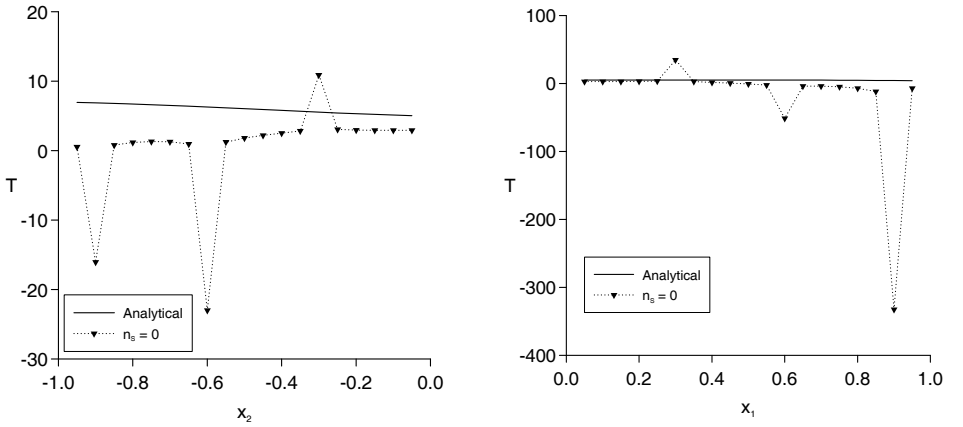

Figure 3: Analytical (—) and numerical ($\cdots\blacktriangledown\cdots$) temperatures (a) $\mathrm{T}|_{\mathrm{EO}}$, and (b) $\mathrm{T}|_{\mathrm{OA}}$, obtained using the LSM without subtracting any singular solutions/eigenfunctions ($\mathrm{n_S} = 0$) and $p_{\mathrm{T}} = 1\%$ noise added into the boundary temperature $\mathrm{T}|_{\Gamma_{\mathrm{D}}}$, for the N-N singular direct problem given by Example 1.

for the temperature and normal heat flux, respectively, where $\widetilde{\Gamma}$ denotes the set of boundary collocation points, since on using these errors divisions by zero and very high errors at points where the temperature and/or normal heat flux have relatively small values are avoided.

7.3 Direct problem subjected to noisy data

If the LSM is applied to solving a singular direct problem for the steady-state heat conduction subjected to noisy data without subtracting any singular solutions/eigenfunctions ($\mathrm{n_S} = 0$) then the numerical solution retrieved by this direct solution method is not only inaccurate, but also unstable. This aspect, which is strongly related to the direct solution method for the perturbed direct problem for the Laplace equation, can be clearly noticed from Figs. 3(a) and (b) that present the analytical and LSM-based numerical temperatures on the wedges EO and OA, respectively, when the Dirichlet data $\mathrm{T}|_{\Gamma_{\mathrm{D}}} = \mathrm{T}|_{\mathrm{AB}\cup\mathrm{CD}}$ was perturbed by $p_{\mathrm{T}} = 1\%$ noise, in the case of Example 1.

Figs. 4(a)-(d) illustrate a comparison between the analytical and numerical solutions for $\mathrm{T}|_{\mathrm{EO}}$ obtained by removing various numbers of singular functions/eigenfunctions, namely $\mathrm{n_S} = 1$, $\mathrm{n_S} = 3$, $\mathrm{n_S} = 5$ and $\mathrm{n_S} = 6$, respectively, for Example 1. It can be seen from these figures that, although by solving this problem using the LSM and accounting for the appropriate singular solutions/eigenfunctions, i.e. $\mathrm{n_S} \geq 1$, the

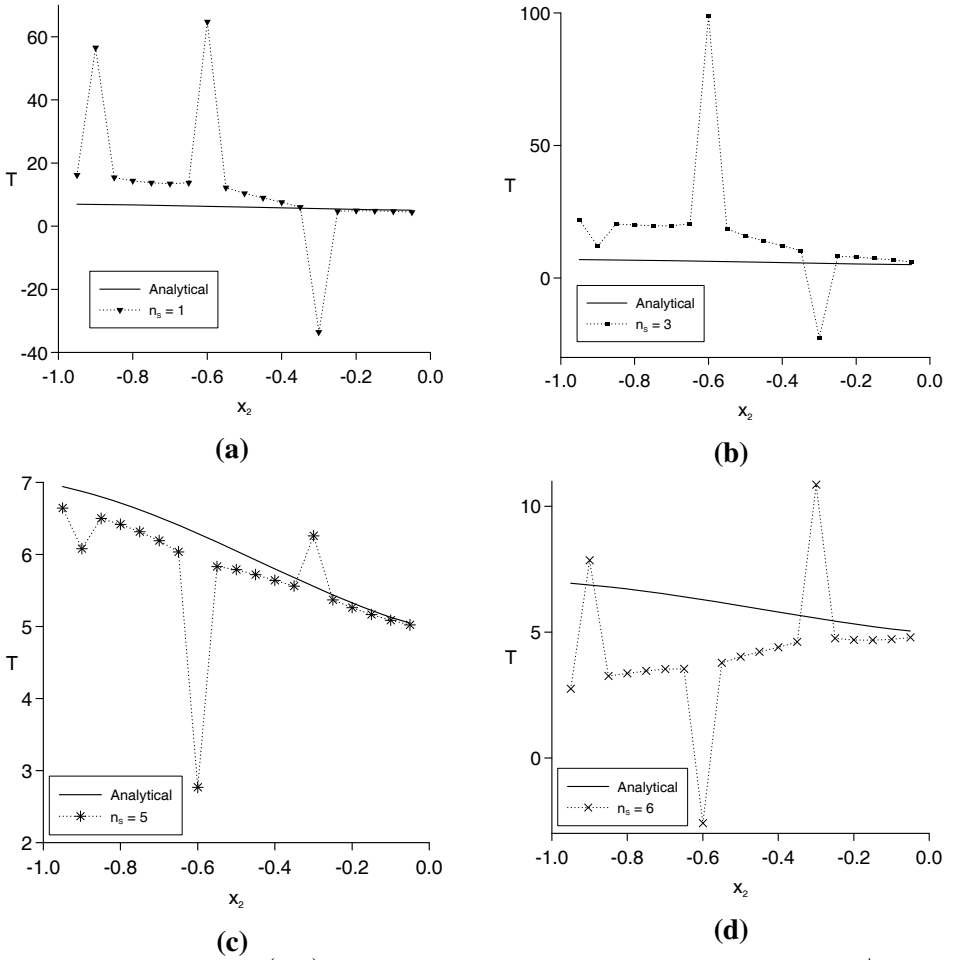

Figure 4: Analytical (—) and numerical values for the temperature $T|_{EO}$, obtained using the LSM, $p_T = 1\%$ noise added into the boundary temperature $T|_{\Gamma_D}$ and subtracting various numbers of singular solutions/eigenfunctions, namely $n_S = 1\,(\cdots\blacktriangledown\cdots)$, $n_S = 3\,(\cdots\bullet\cdots)$, $n_S = 5\,(\cdots*\cdots)$ and $n_S = 6\,(\cdots\times\cdots)$, for the singular direct problem given by Example 1.

numerical results are improved (especially in the vicinity of the singular point O), the numerically retrieved solutions for the temperature and normal heat flux still suffer from the point of view of the accuracy and stability. In this case, inaccurate numerical results are also obtained for the exact flux intensity factors given by equation (50.4), as can be seen from Table 1, which presents the numerical values, $\alpha_{\rm j}^{(\rm num)}$, for the flux intensity factors, $\alpha_{\rm j}$, as well as the corresponding absolute errors defined as

$$\mathrm{Err}(\alpha_{\rm j}) = |\alpha_{\rm j}^{(\rm num)} - \alpha_{\rm j}|. \tag{56}$$

Table 1: The numerically retrieved values, $\alpha_{\rm j}^{(\rm num)}$, for the flux intensity factors and the corresponding absolute errors, $\mathrm{Err}(\alpha_{\rm j})$, obtained using the LSM, $p_{\rm T} = 1\%$ noise added into the boundary temperature $\mathrm{T}|_{\Gamma_{\rm D}}$ and subtracting various numbers of singular solutions/eigenfunctions, namely $\mathrm{n_S} = 1$, $\mathrm{n_S} = 3$, $\mathrm{n_S} = 5$ and $\mathrm{n_S} = 6$, for the N-N singular direct problem given by Example 1.

$\mathrm{n_S}$	$\alpha_1^{(\rm num)}$	$\mathrm{Err}(\alpha_1)$	$\alpha_2^{(\rm num)}$	$\mathrm{Err}(\alpha_2)$	$\alpha_3^{(\rm num)}$	$\mathrm{Err}(\alpha_3)$	$\alpha_4^{(\rm num)}$	$\mathrm{Err}(\alpha_4)$
1	−3.76	3.76	–	–	–	–	–	–
3	−2.37	2.37	2.23	0.27	−1.24	0.26	–	–
5	0.19	0.19	2.49	0.01	−1.54	0.04	−2.01	0.01
6	1.97	1.97	2.93	0.43	−1.61	0.11	−2.72	0.72

The aforementioned inconvenience can be overcome by solving the MFS+SST system of linear algebraic equations (38) for the perturbed singular direct problem given by Example 1, in conjunction with one of the regularization methods described in the previous section, namely the TRM or SVD, together with the L-curve criterion for selecting the optimal value for the regularization parameter. Figs. 5(a) and (b) illustrate the analytical and numerical results for the temperatures on the wedges EO and OA, respectively, retrieved by employing the TRM, in conjunction with the L-curve criterion for choosing the optimal regularization parameter, $\mathrm{n_S} = 6$ and various values of noise added into the Dirichlet data $\mathrm{T}|_{\Gamma_{\rm D}} = \mathrm{T}|_{\rm AB\cup CD}$, in the case of Example 1. On comparing Figs. 3, 4 and 5(a)-(b), we can conclude that the TRM provides very accurate MFS+SST-based numerical solutions to singular direct problems subjected to noisy boundary data, at the same time having a regularizing/stabilizing effect on the MFS+SST solutions to such problems. The same conclusion can also be drawn from Figs. 5(c) and (d) which present the results

shown in Figs. 5(a) and (b) in terms of the normalized errors $\mathrm{err}(\mathrm{T}(\mathbf{x}))$, $\mathbf{x} \in \mathrm{EO}$, and $\mathrm{err}(\mathrm{T}(\mathbf{x}))$, $\mathbf{x} \in \mathrm{OA}$, respectively, as defined by formula (55).

The SVD, in conjunction with the L-curve method for selecting the optimal truncation number $\mathrm{n_{opt}}$, also provides very accurate and stable results with respect to decreasing the level of noise added into the boundary temperature $\mathrm{T}|_{\Gamma_\mathrm{D}} = \mathrm{T}|_{\mathrm{AB}\cup\mathrm{CD}}$, for the N-N singular direct problem described in Example 1. The analytical and SVD-based numerical results for the temperatures $\mathrm{T}|_{\mathrm{EO}}$ and $\mathrm{T}|_{\mathrm{OA}}$ are shown in Figs. 6(a) and (b), respectively, whilst Figs. 6(c) and (d) present the corresponding normalized errors for the numerical temperatures retrieved on the N-N wedges EO and OA, respectively.

Table 2 tabulates the relative RMS errors, $\mathrm{e_T}(\Gamma \setminus \Gamma_\mathrm{D})$ and $\mathrm{e}_\phi(\Gamma \setminus \Gamma_\mathrm{N})$, and the corresponding optimal regularization parameters, $\mathrm{n_{opt}}$ or λ_{opt}, obtained using the LSM, SVD and TRM, $\mathrm{n_S} = 6$ and various amounts of noise added into the temperature boundary data, for the N-N singular direct problem given by Example 1. From this table, as well as Figs. $4-6$, we can conclude that both the TRM and SVD, in conjunction with the L-curve method for selecting the corresponding optimal regularization parameter, have a regularizing/stabilizing character for the combined MSF and SST scheme, at the same time improving significantly the accuracy of the numerical solutions, in the case of the N-N singular direct problem given by Example 1 subjected to noisy boundary temperature. It should be noted that, in terms of accuracy, both regularization methods employed in this study have the same effect on the numerical solutions to perturbed singular direct problems.

The same accurate and stable numerical results have been obtained for the N-D singular direct problem given by Example 2 when the input Neumann data on Γ_N has been perturbed by additive Gaussian noise. The analytical and numerical results for the normal heat flux and temperature on the wedges adjacent to the singularity O, obtained using the MFS+SST scheme, in conjunction with the TRM and SVD, are illustrated in Figs 7(a) and (b), and Figs 8(a) and (b), respectively. The effect of the TRM and SVD on the accuracy of the numerical results in comparison with the LSM is clearly shown in Table 3, which presents the relative RMS errors, $\mathrm{e_T}(\Gamma \setminus \Gamma_\mathrm{D})$ and $\mathrm{e}_\phi(\Gamma \setminus \Gamma_\mathrm{N})$, and the values for the corresponding optimal regularization parameters, $\mathrm{n_{opt}}$ or λ_{opt}, obtained using the LSM, SVD and TRM, $\mathrm{n_S} = 6$ and various levels of noise added into $\phi|_{\Gamma_\mathrm{N}}$, for Example 2.

7.4 Inverse problem subjected to noisy data

Consider now the D-N singular inverse problem given by Example 3 with perturbed boundary temperature on Γ_D. This singular problem is actually more severe than the singular direct problems with noisy boundary data, in the sense that apart from the singularity due to the abrupt change in boundary conditions on the side DA (in

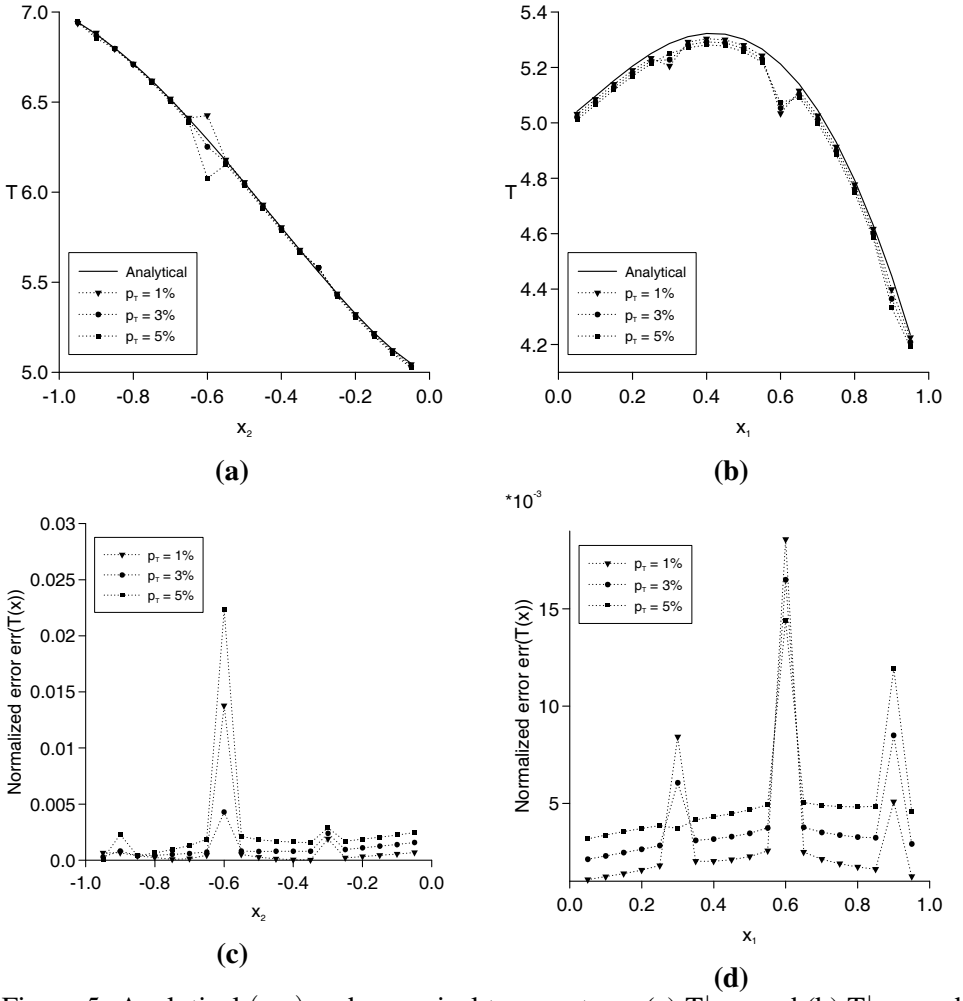

Figure 5: Analytical (—) and numerical temperatures (a) $\mathrm{T}|_{\mathrm{EO}}$, and (b) $\mathrm{T}|_{\mathrm{OA}}$, and the corresponding normalized errors (c) $\mathrm{err}(\mathrm{T}(\mathbf{x}))$, $\mathbf{x} \in$ EO, and (d) $\mathrm{err}(\mathrm{T}(\mathbf{x}))$, $\mathbf{x} \in$ OA, obtained using the TRM, λ_{opt} chosen according to the L-curve criterion, subtracting $\mathrm{n_S} = 6$ singular solutions/eigenfunctions and various levels of noise added into the boundary temperature $\mathrm{T}|_{\Gamma_{\mathrm{D}}}$, namely $p_{\mathrm{T}} = 1\%\,(\cdots\blacktriangledown\cdots)$, $p_{\mathrm{T}} = 3\%\,(\cdots\bullet\cdots)$ and $p_{\mathrm{T}} = 5\%\,(\cdots\blacksquare\cdots)$, for the N-N singular direct problem given by Example 1.

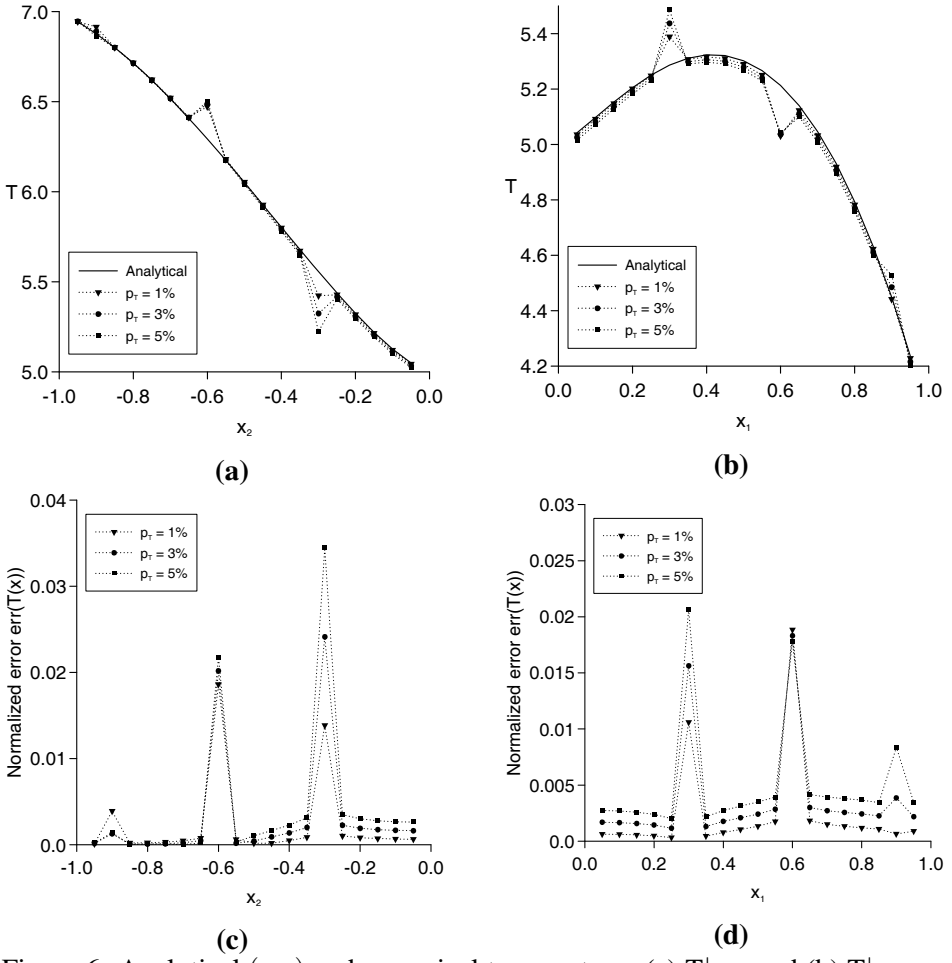

Figure 6: Analytical (—) and numerical temperatures (a) $T|_{EO}$, and (b) $T|_{OA}$, and the corresponding normalized errors (c) $\mathrm{err}(T(\mathbf{x}))$, $\mathbf{x} \in$ EO, and (d) $\mathrm{err}(T(\mathbf{x}))$, $\mathbf{x} \in$ OA, obtained using the SVD, n_{opt} chosen according to the L-curve criterion, subtracting $n_S = 6$ singular solutions/eigenfunctions and various levels of noise added into the boundary temperature $T|_{\Gamma_D}$, namely $p_T = 1\%\,(\cdots\blacktriangledown\cdots)$, $p_T = 3\%\,(\cdots\bullet\cdots)$ and $p_T = 5\%\,(\cdots\blacksquare\cdots)$, for the N-N singular direct problem given by Example 1.

Table 2: The relative RMS errors, $e_T(\Gamma \setminus \Gamma_D)$ and $e_\phi(\Gamma \setminus \Gamma_N)$, and the values for the corresponding optimal regularization parameters, n_{opt} or λ_{opt}, obtained using the LSM, SVD and TRM, $n_S = 6$ and various levels of noise added into the boundary temperature $T|_{\Gamma_D}$, for the N-N singular direct problem given by Example 1.

Method	$p_T\|_{\Gamma_D}$	$e_T(\Gamma \setminus \Gamma_D)$	$e_\phi(\Gamma \setminus \Gamma_N)$	n_{opt}/λ_{opt}
LSM	1%	0.94733×10^{0}	0.57505×10^{0}	–
	3%	0.29226×10^{1}	0.17250×10^{1}	–
	5%	0.48720×10^{1}	0.28750×10^{1}	–
SVD	1%	0.50002×10^{-2}	0.93940×10^{-3}	14
	3%	0.67140×10^{-2}	0.13848×10^{-2}	14
	5%	0.88853×10^{-2}	0.32013×10^{-2}	14
TRM	1%	0.43086×10^{-2}	0.29648×10^{-2}	1.0×10^{-1}
	3%	0.47218×10^{-2}	0.31985×10^{-2}	1.0×10^{-1}
	5%	0.70128×10^{-2}	0.39149×10^{-2}	1.0×10^{-1}

Table 3: The relative RMS errors, $e_T(\Gamma \setminus \Gamma_D)$ and $e_\phi(\Gamma \setminus \Gamma_N)$, and the values for the corresponding optimal regularization parameters, n_{opt} or λ_{opt}, obtained using the LSM, SVD and TRM, $n_S = 6$ and various levels of noise added into the normal heat flux through the boundary $p_\phi|_{\Gamma_N}$, for the N-D singular direct problem given by Example 2.

Method	$p_\phi\|_{\Gamma_N}$	$e_T(\Gamma \setminus \Gamma_D)$	$e_\phi(\Gamma \setminus \Gamma_N)$	n_{opt}/λ_{opt}
LSM	1%	0.99454×10^{-1}	0.34197×10^{0}	–
	3%	0.29835×10^{0}	0.10259×10^{1}	–
	5%	0.49726×10^{0}	0.17098×10^{1}	–
SVD	1%	0.97503×10^{-3}	0.84285×10^{-2}	13
	3%	0.32706×10^{-3}	0.28098×10^{-2}	13
	5%	0.16230×10^{-2}	0.14047×10^{-1}	13
TRM	1%	0.19742×10^{-3}	0.16317×10^{-2}	1.0×10^{-3}
	3%	0.57438×10^{-3}	0.53492×10^{-2}	1.0×10^{-3}
	5%	0.11378×10^{-2}	0.93756×10^{-2}	1.0×10^{-3}

this case, $T|_{OA}$ and $\phi|_{DO}$ are known), see Fig. 2(c), it is also ill-posed since both the temperature and normal heat flux are prescribed on AB $\cup$ CD, whilst neither the temperature, nor the normal heat flux is prescribed on the boundary BC, see e.g. Hadamard (1923). Although not presented, it is reported that, as expected, the LSM

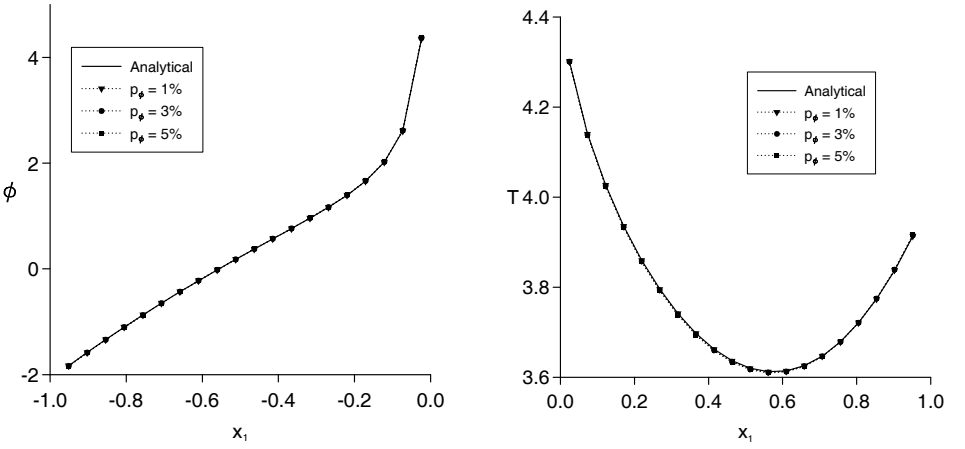

Figure 7: Analytical (—) and numerical values for (a) the normal heat flux $\phi|_{\mathrm{DO}}$, and (b) the temperature $\mathrm{T}|_{\mathrm{OA}}$, obtained using the TRM, λ_{opt} chosen according to the L-curve criterion, subtracting $\mathrm{n_S} = 6$ singular solutions/eigenfunctions and various levels of noise added into the normal heat flux through the boundary $\phi|_{\Gamma_{\mathrm{N}}}$, namely $p_\phi = 1\%\,(\cdots\blacktriangledown\cdots)$, $p_\phi = 3\%\,(\cdots\bullet\cdots)$ and $p_\phi = 5\%\,(\cdots\blacksquare\cdots)$, for the N-D singular direct problem given by Example 2.

in conjunction with the SST, as well as the TRM and SVD without subtracting the singular solutions/eigenfunctions, provide us with highly unstable and inaccurate numerical results for the temperature and flux not only on the wedges adjacent to the singularity, but also on the under-specified boundary BC. Therefore, both the SST and regularization are required to stably solve the inverse problem under investigation.

Figs. 9(a) and (b) present the numerical solutions for the temperature $\mathrm{T}|_{\mathrm{DO}}$ and normal heat flux $\phi|_{\mathrm{OA}}$, respectively, retrieved by the TRM along with the L-curve criterion, subtracting $\mathrm{n_S} = 6$ singular functions and various levels of noise added into the boundary temperature $\mathrm{T}|_{\Gamma_{\mathrm{D}}}$, in comparison with their analytical counterparts, for the D-N singular inverse problem given by Example 3. It can be seen from these figures, as well as Figs. 9(c) and (d), which show the associated normalized errors $\mathrm{err}(\mathrm{T}(\mathbf{x}))$, $\mathbf{x} \in \mathrm{DO}$, and $\mathrm{err}(\phi(\mathbf{x}))$, $\mathbf{x} \in \mathrm{OA}$, that the numerical results for both the temperature $\mathrm{T}|_{\mathrm{DO}}$ and normal heat flux $\phi|_{\mathrm{OA}}$ on the wedges adjacent to the singular point O are in excellent agreement with their corresponding analytical values, being at the same time exempted from high and unbounded oscillations.

The numerical temperature and normal heat flux on the under-specified boundary

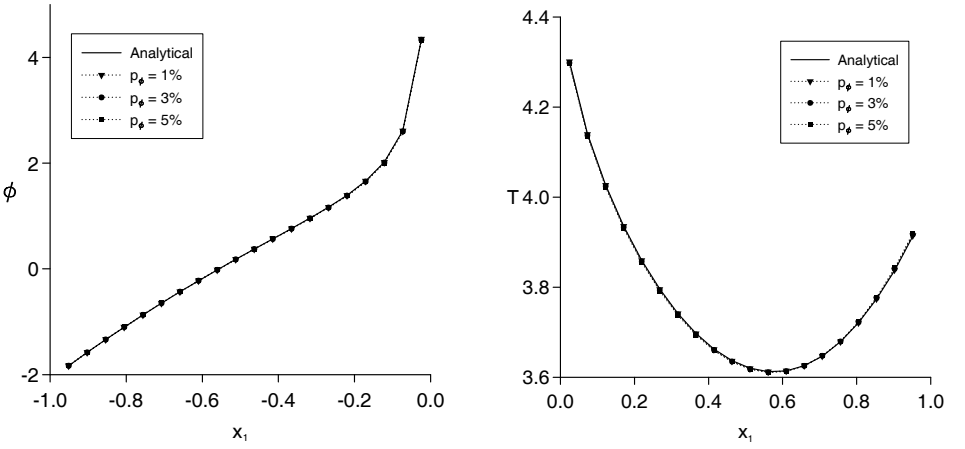

(a) **(b)**

Figure 8: Analytical (—) and numerical values for (a) the normal heat flux $\phi|_{\mathrm{DO}}$, and (b) the temperature $\mathrm{T}|_{\mathrm{OA}}$, obtained using the SVD, $\mathrm{n_{opt}}$ chosen according to the L-curve criterion, subtracting $\mathrm{n_S} = 6$ singular solutions/eigenfunctions and various levels of noise added into the normal heat flux through the boundary $\phi|_{\Gamma_{\mathrm{N}}}$, namely $p_\phi = 1\%\,(\cdots\blacktriangledown\cdots)$, $p_\phi = 3\%\,(\cdots\bullet\cdots)$ and $p_\phi = 5\%\,(\cdots\blacksquare\cdots)$, for the N-D singular direct problem given by Example 2.

BC, obtained using the regularized MFS+SST, $\mathrm{n_S} = 6$ and $p_{\mathrm{T}} \in \{1\%, 3\%, 5\%\}$, are illustrated in Figs. 10(a) and (b). From these figures we can conclude that the numerical results for the temperature and normal heat flux on the under-specified boundary BC are also excellent approximations for their corresponding exact values and, in addition, they are convergent and stable with respect to decreasing the amount of noise added into the input boundary temperature $\mathrm{T}|_{\mathrm{D}}$.

Accurate, stable and convergent results are also obtained for the unknown temperature $\mathrm{T}|_{\mathrm{DO}}$ and normal heat flux $\phi|_{\mathrm{OA}}$, as well as the unspecified temperature $\mathrm{T}|_{\mathrm{BC}}$ and normal heat flux $\phi|_{\mathrm{BC}}$, when the MFS+SST, in conjunction with the SVD and the L-curve criterion, is employed to numerically solve the singular inverse problem given by Example 3 subjected to perturbed input boundary temperature, as can be observed form Figs. 11 and 12, respectively. By comparing Figs. $9-12$, it can be noticed that, although the normalized errors for the numerical temperature $\mathrm{T}|_{\mathrm{BC}\cup\mathrm{DO}}$ and normal heat flux $\phi|_{\mathrm{OA}\cup\mathrm{BC}}$ obtained using the TRM and SVD are of the same order of magnitude, the TRM-based numerical solutions for the temperature and normal heat flux are slightly more inaccurate than those retrieved using the SVD. This quantitative result is also valid for the relative RMS errors $\mathrm{e_T(BC)}$ and $\mathrm{e}_\phi\mathrm{(BC)}$ presented together with the values for the corresponding optimal regu-

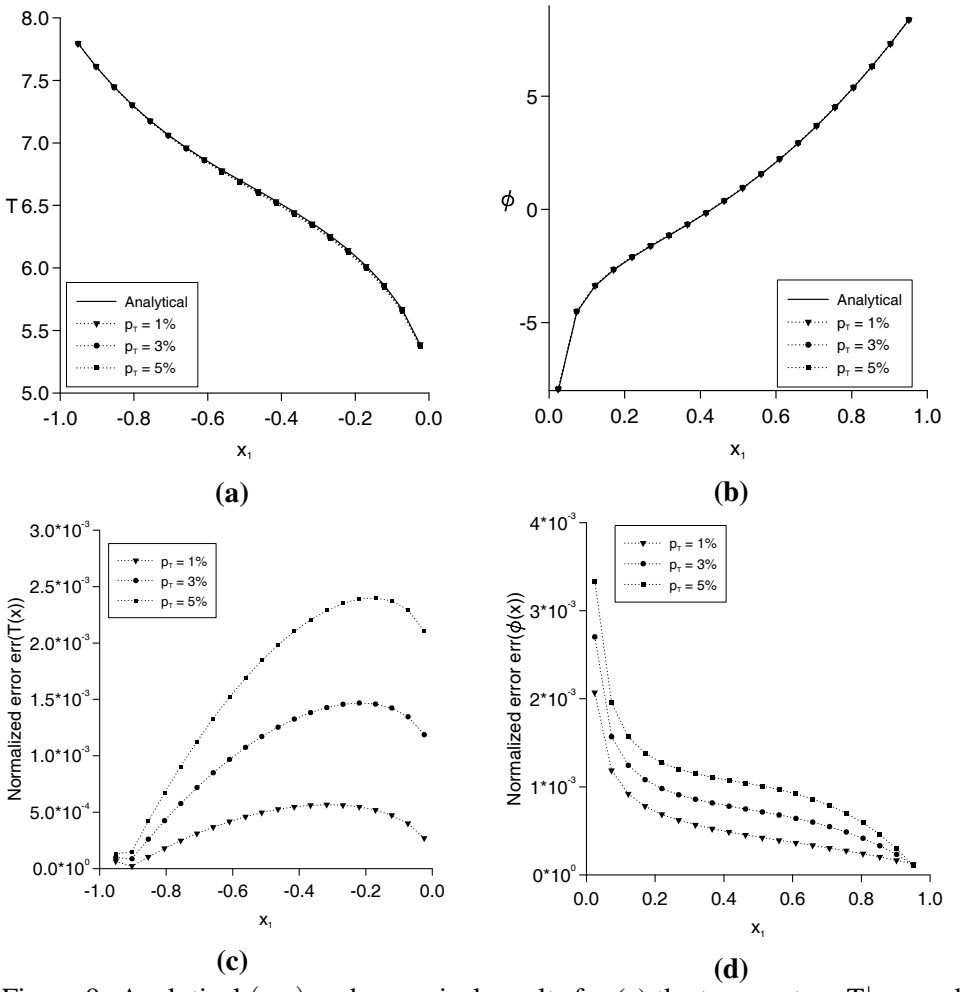

Figure 9: Analytical (—) and numerical results for (a) the temperature $\mathrm{T}|_{\mathrm{DO}}$, and (b) normal heat flux $\phi|_{\mathrm{OA}}$, and the corresponding normalized errors (c) $\mathrm{err}(T(\mathbf{x}))$, $\mathbf{x} \in \mathrm{DO}$, and (d) $\mathrm{err}(\phi(\mathbf{x}))$, $\mathbf{x} \in \mathrm{OA}$, obtained using the TRM, λ_{opt} chosen according to the L-curve criterion, subtracting $\mathrm{n_S} = 6$ singular solutions/eigenfunctions and various levels of noise added into the boundary temperature $\mathrm{T}|_{\Gamma_{\mathrm{D}}}$, namely $p_{\mathrm{T}} = 1\%\,(\cdots\blacktriangledown\cdots)$, $p_{\mathrm{T}} = 3\%\,(\cdots\bullet\cdots)$ and $p_{\mathrm{T}} = 5\%\,(\cdots\blacksquare\cdots)$, for the D-N singular inverse problem given by Example 3.

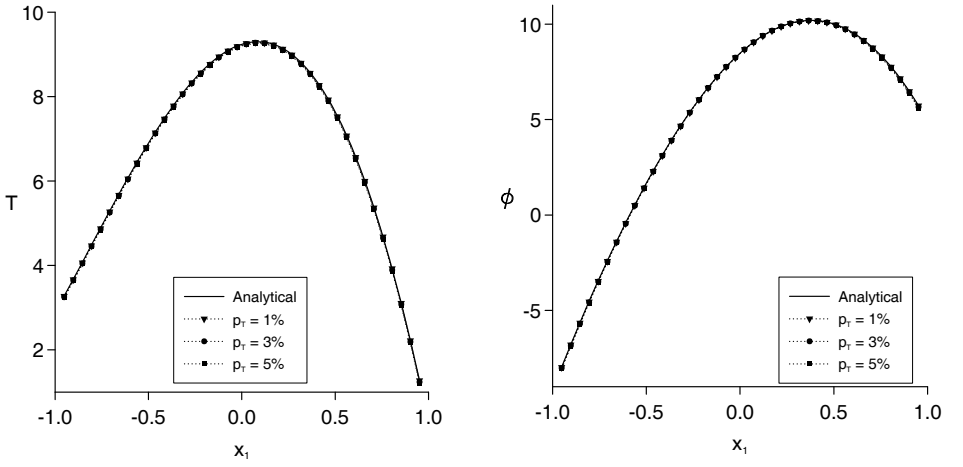

Figure 10: Analytical (—) and numerical results for (a) the temperature $T|_{BC}$, and (b) normal heat flux $\phi|_{BC}$, obtained using the TRM, λ_{opt} chosen according to the L-curve criterion, subtracting $n_S = 6$ singular solutions/eigenfunctions and various levels of noise added into the boundary temperature $T|_{\Gamma_D}$, namely $p_T = 1\%\,(\cdots\blacktriangledown\cdots)$, $p_T = 3\%\,(\cdots\bullet\cdots)$ and $p_T = 5\%\,(\cdots\blacksquare\cdots)$, for the D-N singular inverse problem given by Example 3.

larization parameters n_{opt} or λ_{opt} in Table 4, as well as the numerical flux intensity factors listed in Table 5.

Overall, from the numerical results presented in this section it can be concluded that the MFS+SST proposed in Section 5, combined with any of the regularization methods described in Section 4, i.e. the TRM and SVD, is a very suitable method for solving both direct and inverse boundary value problems exhibiting singularities caused by the presence of sharp corners in the boundary of the solution domain and/or abrupt changes in the boundary conditions, for the isotropic two-dimensional isotropic steady-state heat conduction problem with noisy boundary data. The numerical temperatures and normal heat fluxes retrieved using this regularized MFS+SST are very good approximations for their analytical values on the entire boundary, they are exempted from oscillations in the neighbourhood of the singular point and there is no need of further mesh refinement in the vicinity of the singularities.

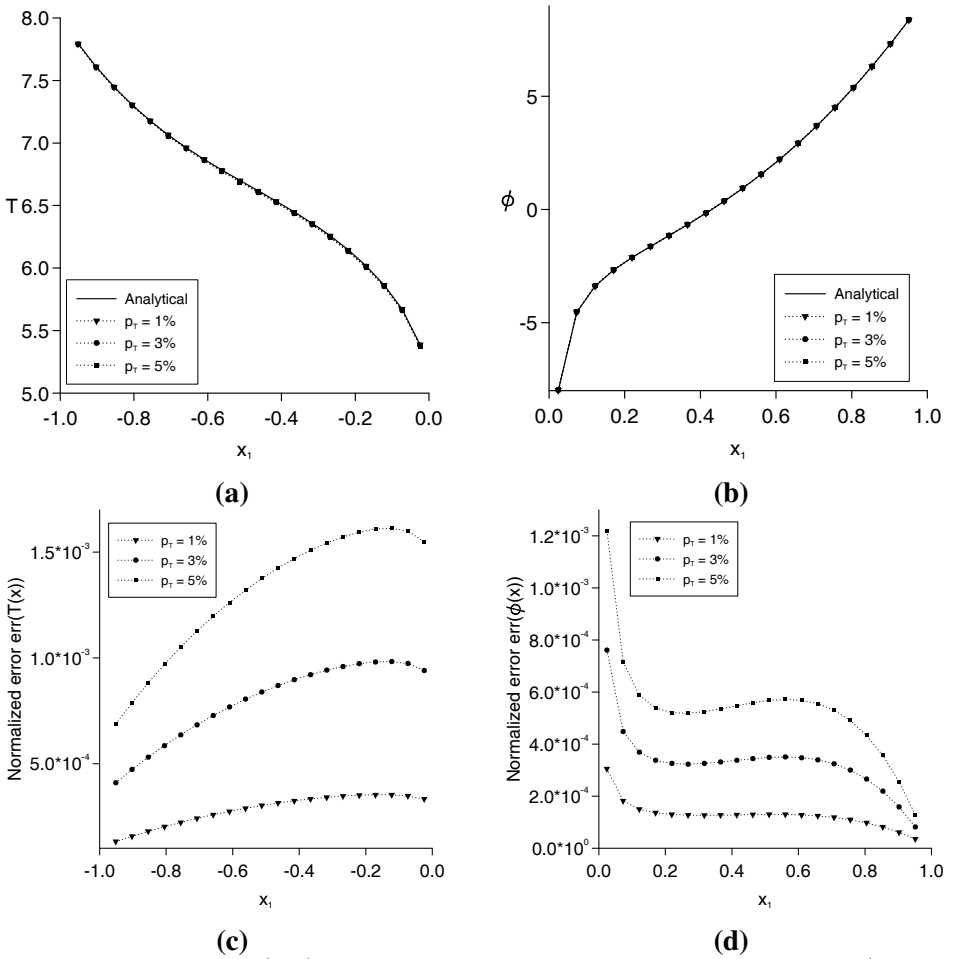

Figure 11: Analytical (—) and numerical results for (a) the temperature $T|_{DO}$, and (b) normal heat flux $\phi|_{OA}$, and the corresponding normalized errors (c) $\mathrm{err}(T(\mathbf{x}))$, $\mathbf{x} \in$ DO, and (d) $\mathrm{err}(\phi(\mathbf{x}))$, $\mathbf{x} \in$ OA, obtained using the SVD, n_{opt} chosen according to the L-curve criterion, subtracting $n_S = 6$ singular solutions/eigenfunctions and various levels of noise added into the boundary temperature $T|_{\Gamma_D}$, namely $p_T = 1\%\,(\cdots\blacktriangledown\cdots)$, $p_T = 3\%\,(\cdots\bullet\cdots)$ and $p_T = 5\%\,(\cdots\blacksquare\cdots)$, for the D-D singular inverse problem given by Example 3.

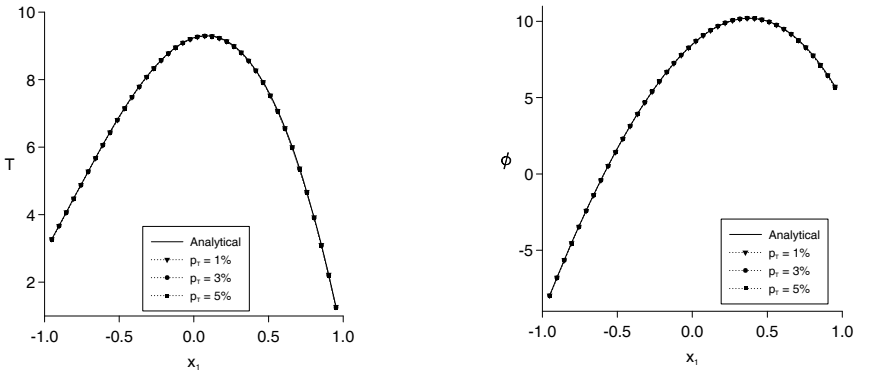

(a) **(b)**

Figure 12: Analytical (—) and numerical results for (a) the temperature $T|_{BC}$, and (b) normal heat flux $\phi|_{BC}$, obtained using the SVD, n_{opt} chosen according to the L-curve criterion, subtracting $n_S = 6$ singular solutions/eigenfunctions and various levels of noise added into the boundary temperature $T|_{\Gamma_D}$, namely $p_T = 1\%\,(\cdots\blacktriangledown\cdots)$, $p_T = 3\%\,(\cdots\bullet\cdots)$ and $p_T = 5\%\,(\cdots\blacksquare\cdots)$, for the D-D singular inverse problem given by Example 3.

Table 4: The relative RMS errors, $e_T(BC)$ and $e_\phi(BC)$, and the values for the corresponding optimal regularization parameters, n_{opt} or λ_{opt}, obtained using the LSM, SVD and TRM, $n_S = 6$ and various amounts of noise added into the boundary temperature $T|_{\Gamma_D}$, for the D-N singular inverse problem given by Example 3.

Method	$p_T\|_{\Gamma_D}$	$e_T(BC)$	$e_\phi(BC)$	$n_{opt}\,/\,\lambda_{opt}$
LSM	1%	0.11655×10^{0}	0.25011×10^{0}	–
	3%	0.33497×10^{0}	0.75038×10^{0}	–
	5%	0.55828×10^{0}	0.12506×10^{1}	–
SVD	1%	0.89535×10^{-3}	0.10505×10^{-2}	9
	3%	0.24584×10^{-2}	0.30050×10^{-2}	9
	5%	0.40264×10^{-2}	0.49789×10^{-2}	9
TRM	1%	0.20118×10^{-2}	0.25635×10^{-2}	1.0×10^{-2}
	3%	0.45654×10^{-2}	0.55811×10^{-2}	1.0×10^{-2}
	5%	0.71598×10^{-2}	0.87984×10^{-2}	1.0×10^{-2}

Table 5: The numerically retrieved values, $\alpha_j^{(num)}$, for the flux intensity factors and the corresponding absolute errors, $Err(\alpha_j)$, obtained using the SVD and TRM, $n_S = 6$ and various levels of noise added into the boundary temperature $T|_{\Gamma_D}$, for the D-N singular inverse problem given by Example 3.

Method	p_T	$\alpha_1^{(num)}$	$Err(\alpha_1)$	$\alpha_2^{(num)}$	$Err(\alpha_2)$	$\alpha_3^{(num)}$	$Err(\alpha_3)$	$\alpha_4^{(num)}$	$Err(\alpha_4)$
SVD	1%	2.4979	0.0021	−0.00153	0.00153	−1.5005	0.0005	−2.0007	0.0007
	3%	2.4946	0.0054	−0.00415	0.00415	−1.5019	0.0019	−2.0018	0.0018
	5%	2.4913	0.0087	−0.00677	0.00677	−1.5034	0.0034	−2.0030	0.0030
TRM	1%	2.4860	0.0140	−0.00471	0.00471	−1.4999	0.0001	−2.0011	0.0011
	3%	2.4814	0.0186	−0.01193	0.01193	−1.4979	0.0021	−2.0020	0.0020
	5%	2.4769	0.0231	−0.01914	0.01914	−1.5028	0.0028	−2.0029	0.0029

8 Conclusions

In this paper, the MFS was applied for solving accurately and stably direct and inverse problems associated with the two-dimensional isotropic steady-state heat conduction (Laplace equation) in the presence of boundary singularities and noisy boundary data. The existence of the boundary singularity was accounted for by subtracting from the original MFS solution the corresponding singular solutions/eigenfunctions, as given by the asymptotic expansion of the solution near the singular point. Hence, in addition to the original MFS unknowns, new unknowns were introduced, namely the so-called flux intensity factors. Consequently, the original MFS system was extended by considering a number of additional equations which equals the number of flux intensity factors introduced and specifically imposes the type of singularity analysed in the vicinity of the singular point. However, even in the case when the boundary singularity was taken into account, the numerical solutions obtained by the direct inversion of the associated MFS linear algebraic system were found to be inaccurate and unstable, provided that the given boundary temperature and/or normal heat flux were contaminated by noise. This inconvenience was overcome for the direct and inverse problems investigated in this study by employing either the TRM or SVD. The corresponding optimal regularization parameter, namely the optimal regularization parameter in the case of the TRM and the optimal truncation number for the SVD, was chosen according to Hansen's L-curve criterion. The proposed MFS+SST, together with the aforementioned regularization methods, was implemented and analysed for noisy direct and inverse problems in two-dimensional domains containing an edge crack or a V-notch, as well as an L-shaped domain.

From the numerical results presented in this study, we can conclude that the advantages of the proposed method over other well known methods, such as mesh refinement in the neighbourhood of the singularity, the use of singular BEMs and/or FEMs etc., are the high accuracy which can be obtained even when employing a small number of collocation points and sources, and the simplicity of the computational scheme. A possible drawback of the present method is the difficulty in extending the method to deal with singularities in three-dimensional problems since such an extension is not straightforward.

References

Apel; T., Nicaise, S. (1998): The finite element method with anisotropic mesh grading for elliptic problems in domains with corners and edges. *Mathematical Methods in Applied Sciences*, vol. 21, pp. 519–549.

Apel, T.; Sändig, A.-M.; Whiteman, J.R. (1996): Graded mesh refinement and

error estimates for finite element solution of elliptic boundary value problems in non-smooth domains. *Mathematical Methods in the Applied Sciences*, vol. 19, pp.63–85.

Berger, J.R.; Karageorghis, A. (1999): The method of fundamental solutions for heat conduction in layered materials. *International Journal for Numerical Methods in Engineering*, vol. 45, pp. 1681–1694.

Berger, J.R.; Karageorghis, A. (2001): The method of fundamental solutions for layered elastic materials. *Engineering Analysis with Boundary Elements*, vol. 25, pp. 877–886.

Cannon, J.R. (1964): The numerical solution of the Dirichlet problem for Laplace equation by linear programming. *SIAM Journal on Applied Mathematics*, vol. 12, pp. 233–237.

Castellanos, J.L.; Gomez, S.; Guerra, V. (2002): The triangle method for finding the corner of the L-curve. *Applied Numerical Mathematics*, vol. 43, pp. 359–373.

Chen, L.Y.; Chen, J.T.; Hong, H.K.; Chen, C.H. (1995): Application of Cesàro mean and the L-curve for the dconvolution problem, *Soil Dynamics Earthquake Engineering*, vol. 14, pp. 361–373.

Elliotis, M.; Georgiou, G.; Xenophontos, C. (2002): The solution of Laplacian problems over L-shaped domains with a singular function boundary integral method. *Communications in Numerical Methods in Engineering*, vol. 18, pp. 213–222.

Engl, H.W.; Hanke, M.; Neubauer, A. (2000): *Regularization of Inverse Problems*, Kluwer Academic, Dordrecht.

Fairweather, G.; Karageorghis, A. (1998): The method of fundamental solutions for elliptic boundary value problems. *Advances in Computational Mathematics*, vol. 9, pp. 69–95.

Golberg, M.A.; Chen, C.S. (1999): The method of fundamental solutions for potential, Helmholtz and diffusion problems. In: M.A. Golberg (ed.) *Boundary Integral Methods: Numerical and Mathematical Aspects*, WIT Press and Computational Mechanics Publications, Boston, pp. 105–176.

Guerra, V.; Hernandez, V. (2001): Numerical aspects in locating the corner of the L-curve. In: M. Lassonde (ed.) *Approximation, Optimization and Mathematical Economics*, Springer-Verlag, Heidelberg, pp. 121–131.

Hadamard, J. (1923): *Lectures on Cauchy Problem in Linear Partial Differential Equations*, Yale University Press, New Haven.

Hanke, M. (1996): Limitations of the L-curve method in ill-posed problems. *BIT*, vol. 36, pp. 287–301.

Hansen, P.C. (1998): *Rank-Deficient and Discrete Ill-Posed Problems: Numerical Aspects of Linear Inversion*, SIAM, Philadelphia.

Hon, Y.C.; Wei, T. (2004): A fundamental solution method for inverse heat conduction problems. *Engineering Analysis with Boundary Elements*, vol. 28, pp. 489–495.

Hon, Y.C.; Wei, T. (2005): The method of fundamental solutions for solving multidimensional heat conduction problems. *CMES: Computer Modeling in Engineering & Sciences*, vol. 7, pp. 119-132.

Hu, S.P.; Young, D.L.; Fan, C.M. (2008): FDMFS for diffusion equation with unsteady forcing function. *CMES: Computer Modeling in Engineering & Sciences*, vol. 24, pp. 1-20.

Ingham, D.B.; Heggs, P.J.; Manzoor, M. (1981): The numerical solution of plane potential problems by improved boundary integral equation methods. *Journal of Computational Physics*, vol. 42, pp. 77–98.

Ingham, D.B.; Yuan, Y. (1994): Boundary element solutions of the steady state, singular, inverse heat transfer equation, *International Journal of Heat and Mass Transfer*, vol. 37, pp. 273–280.

Jaswon, M.A.; Symm, G.T. (1977): *Integral Equation Methods in Potential Theory and Elastostatics*, Academic Press, London.

Jin, B.T. (2004): A meshless method for the Laplace and biharmonic equations subjected to noisy data. *CMES: Computer Modeling in Engineering & Sciences*, vol. 6, pp. 253–261.

Jin, B.T.; Marin, L. (2007): The method of fundamental solutions for inverse source problems associated with the steady-state heat conduction. *International Journal for Numerical Methods in Engineering*, vol. 69, pp. 1570–1589.

Jin, B.T.; Zheng, Y. (2006): A meshless method for some inverse problems associated with the Helmholtz equation. *Computer Methods in Applied Mechanics and Engineering*, vol. 195, pp. 2270–2280.

Karageorghis, A. (1992): Modified methods of fundamental solutions for harmonic and biharmonic problems with boundary singularities. *Numerical Methods for Partial Differential Equations*, vol. 8, pp. 1–19.

Karageorghis, A.; Fairweather, G. (1987): The method of fundamental solutions for the numerical solution of the biharmonic equation. *Journal of Computational Physics*, vol. 69, pp. 434–459.

Karageorghis, A.; Fairweather, G. (2000): The method of fundamental solutions for axisymmetric elasticity problems. *Computational Mechanics*, vol. 25, pp. 524–532.

Kaufman, L.; Neumaier, A. (1996): PET regularization by envelope guided conjugate gradients, *IEEE Transactions on Medical Imaging*, vol. 15, pp. 385–389.

Kupradze, V.D.; Aleksidze, M.A. (1964): The method of functional equations for the approximate solution of certain boundary value problems. *USSR Computational Mathematics and Mathematical Physics*, vol. 4, pp. 82–126.

Lefeber, D. (1989): *Solving Problems with Singularities Using Boundary Elements*, CMP, London.

Lesnic, D.; Elliott, L.; Ingham, D.B. (1995): Treatment of singularities in time dependent problems using the boundary element method. *Engineering Analysis with Boundary Elements*, vol. 16, pp. 65–70.

Lesnic, D.; Elliott, L.; Ingham, D.B. (1998): The boundary element method solution of the Laplace and biharmonic equations subjected to noisy boundary data. *International Journal for Numerical Methods in Engineering*, vol. 43, pp. 479–492.

Li, Z.-C.; Lu, T.T. (2000): Singularities and treatments of elliptic boundary value problems. *Mathematical and Computer Modelling*, vol. 31, pp. 97–145.

Liu, C.-S. (2008): Improving the ill-conditioning of the method of fundamental solutions for 2D Laplace equation. *CMES: Computer Modeling in Engineering & Sciences*, vol. 28, pp. 77-93.

Marin, L.; Lesnic, D. (2004): The method of fundamental solutions for the Cauchy problem in two-dimensional linear elasticity. *International Journal of Solids and Structures*, vol. 41, pp. 3425–3438.

Marin, L. (2005a): A meshless method for solving the Cauchy problem in three-dimensional elastostatics. *Computers & Mathematics with Applications*, vol. 50, pp. 73–92.

Marin, L. (2005b): Numerical solutions of the Cauchy problem for steady-state heat transfer in two-dimensional functionally graded materials. *International Journal of Solids and Structures*, vol. 42, pp. 4338–4351.

Marin, L. (2005c): A meshless method for the numerical solution of the Cauchy problem associated with three-dimensional Helmholtz-type equations. *Applied Mathematics and Computation*, vol. 165, pp. 355–374.

Marin, L.; Lesnic, D. (2005): The method of fundamental solutions for the Cauchy problem associated with two-dimensional Helmholtz-type equations, *Computers & Structures* vol. 83, pp. 267–278.

Marin, L. (2008): The method of fundamental solutions for inverse problems associated with the steady-state heat conduction in the presence of sources. *CMES: Computer Modeling in Engineering & Sciences*, vol. 30, pp. 99–122.

Mathon, R.; Johnston, R.L. (1977): The approximate solution of elliptic boundary value problems by fundamental solutions. *SIAM Journal on Numerical Analysis*, vol. 14, pp. 638–650.

Mera, N.S. (2005): The method of fundamental solutions for the backward heat conduction problem. *Inverse Problems in Science and Engineering*, vol. 13, pp. 79–98.

Mera, N.S.; Elliott, L.; Ingham, D.B.; Lesnic, D. (2002): An iterative algorithm for singular Cauchy problems for the steady state heat conduction equation. *Engineering Analysis with Boundary Elements*, vol. 26, pp. 157–168.

Mitic, P.; Rashed, Y.F. (2004): Convergence and stability of the method of meshless fundamental solutions using an array of randomly distributed source. *Engineering Analysis with Boundary Elements*, vol. 28, pp. 143–153.

Morozov, V.A. (1966): On the solution of functional equations by the method of regularization, *Doklady Mathematics*, vol. 7, pp. 414–417.

Motz, H. (1946): The treatment of singularities of partial differential equations by relaxation methods. *Quarterly Journal of Applied Mathematics*, vol. 4, pp. 371–377.

Poullikkas, A.; Karageorghis, A.; Georgiou, G. (1998a): Methods of fundamental solutions for harmonic and biharmonic boundary value problems. *Computational Mechanics*, vol. 21, pp. 416–423.

Poullikkas, A.; Karageorghis, A.; Georgiou, G. (2001): The numerical solution of three-dimensional Signorini problems with the method of fundamental solutions. *Engineering Analysis with Boundary Elements*, vol. 25, pp. 221-227.

Poullikkas, A.; Karageorghis, A.; Georgiou, G. (2002): The numerical solution for three-dimensional elastostatics problems. *Computers & Structures*, vol. 80, pp. 365–370.

Symm, G.T. (1973): Treatment of singularities in the solution of Laplace equation by an integral equation method. *NPL Report NAC 31*.

Tankelevich, R.; Fairweather, G.; Karageorghis, A.; Smyrlis, Y.-S. (2006): Potential field based geometric modeling using the method of fundamental solutions. *International Journal for Numerical Methods in Engineering*, vol. 68, pp. 1257–1280.

Tikhonov, A.N.; Arsenin, V.Y. (1986): *Methods for Solving Ill-Posed Problems*, Nauka, Moscow.

Tsai, C.C. (2001): Meshless BEM for three-dimensional Stokes flow. *CMES: Computer Modeling in Engineering & Sciences*, vol. 3, pp. 117–128.

Tsai, C.C.; Lin, Y.C.; Young, D.L.; Atluri, S.N. (2006): Investigations on the

accuracy and condition number for the method of fundamental solutions. *CMES: Computer Modeling in Engineering & Sciences*, vol. 16, pp. 103-114.

Vogel, C.R. (1996): Non-convergence of the L-curve regularization parameter selection method, *Inverse Problems*, vol. 12, pp. 535–547.

Wahba, G. (1977): Practical approximate solutions to linear operator equations when the data are noisy, *SIAM Journal on Numerical Analysis*, vol. 14, pp. 651–667.

Wait, R.; Mitchell, A.R. (1971): Corner singularities in elliptic problems by finite element methods. *Journal of Computational Physics*, vol. 8, pp. 45–54.

Wait, R. (1978): Finite element methods for elliptic problems with singularities. *Computer Methods in Applied Mechanics and Engineering*, vol. 13, pp. 141–150.

Whiteman, J.R.; Papamichael, N. (1971): Numerical solution of two-dimensional harmonic boundary problems containing singularities by conformal transformation methods. *Report No. TR-2*, Brunel University, Department of Mathematics.

Woods, L.C. (1953): The relaxation treatment of singular points in Poisson's equation. *The Quarterly Journal of Mechanics and Applied Mathematics*, vol. 6, pp. 163–174.

Xenophontos, C.; Elliotis, M.; Georgiou, G. (2006): A singular function boundary integral method for Laplacian problems with boundary singularities. *SIAM Journal on Scientific Computing*, vol. 28, 517–532.

Young, D.L.; Ruan, J.W. (2005): Method of fundamental solutions for scattering problems of electromagnetic waves. *CMES: Computer Modeling in Engineering & Sciences*, vol. 7, pp. 223-232.